Analysis and Design of Reconfigurable and Broadband Microstrip Antenna

Muhammad Qazafi

A Thesis

in

The Department

of

Electrical & Computer Engineering

Presented in Partial Fulfillment of the Requirements
for
Degree of Master of Applied Science (Electrical Engineering)
at
Concordia University, Montreal Quebec, Canada

March 2007

Your file Votre référence
ISBN: 978-0-494-30078-7
Our file Notre référence
ISBN: 978-0-494-30078-7

ABSTRACT

Analysis and Design of Reconfigurable and Broadband Microstrip Antenna

Muhammad Qazafi

This thesis provides several designs of broadband microstrip antennas for the use in WLAN applications. It also highlights the novel reconfigurable microstrip antenna design. The main objective of this thesis is to design a novel microstrip antenna that is broadband, circularly polarized, multiband, reconfigurable and easy-to-fabricate. The thesis, in the first stage, presents a review of various different options available when designing and manufacturing wideband microstrip antennas. The review includes basic theory of microstrip patch antennas, matching techniques and broadbanding techniques. The second stage concentrates on the development of a couple of working prototype antenna designs and finally presents the design of a reconfigurable antenna that can perform over several frequency bands. The shapes of broadband patch antennas used are rectangular, circular and triangular. The multiple resonance technique is used in the design of the broadband antennas. Numerical and measured results are presented and discussed. The proposed patch antennas give measured bandwidth up to 28.5%. The reconfigurable antenna on the other hand is designed to possess frequency and polarization reconfigurability, and can operate in six different frequency bands. In addition to the bandwidth advantage, the proposed configuration offers easy reconfigurability with the ability to exclude switches in the combination part of the feed network. The important aspect of this design is that it provides a high size reduction for all the operating frequencies compared to conventional rectangular patches. Besides

compactness all proposed antennas have gain better than 7dB. The proposed antennas are found to be suitable for WLAN standards.

ACKNOWLEDGEMENT

I wish to thank my advisor Prof. A.R Sebak for his persistent guidance, supervision, professional approach, valuable advice and very inspiring discussions throughout the time he spent with me. I would like to thank INRS-EMT Montreal for the radiation pattern measurements. Without their help I would not be able to finish my research work in time. I would also like to thank Prof. R. Paknys who have provided me a lot of helpful feedback and information, that concern the simulation and measured results. Finally I would like to thank Prof. R. Sedaghati and the the Examining Committee Chair A .Ghrayeb for their kind advises and help.

TABLE OF CONTENTS

LIST OF SYMBOLS

$\overrightarrow{J_b}$	Current density of bottom surface
$\overrightarrow{J_t}$	Current density of top surface
$\overrightarrow{H_a}$	Magnetic field
$\overrightarrow{E_a}$	Electric field
εr	Relative permitivity
ko	Wave number
μ	Permeability of medium
ψ	Eigen function
ω	Radian frequency
$J_m(x)$	Bessel function
k_{mn},	Eigen values
λ	Wave length

LIST OF ABBREVIATIONS

WLAN	Wireless Low Area Network
ISP	Internet Service Provider
ISM	Industrial, Scientific and Medical
FSS	Frequency Selective Surface
PBG	Photonic Band Gap
AUT	Antenna Under Test
MSA	Microstrip Antenna
PCS	Personal Computer System
MMIC	Monolithic Microwave Integrated Circuit
GA	Genetic Algorithm
EMI	Electromagnetic Interference
MoM	Method of Moments

CHAPTER I – INTRODUCTION

1.1 INTRODUCTION

Microstrip antennas have attractive features such as light weight, small volume low profile and low production cost which widely have been researched and developed in the past 20 years [1-4]. Low gain and narrow bandwidth are the two most serious limitations of the microstrip antennas. The compact antenna configuration further degrades these two parameters. This is because of the fact that there is a fundamental relationship between the size, bandwidth and efficiency of an antenna. As antennas are made smaller, either the operating bandwidth or the antenna efficiency must decrease. The gain is also related to the size of the antenna, that is small antennas typically provide lower gain than larger antennas, On the other hand wireless communication has been developed rapidly in the past decade and it has been already had a dramatic impact in our lives. In the last few years, the development of wireless local area networks (WLAN) represented one of the principal interests in the information and communications field. WLAN takes advantage of a license free frequency bands, Industrial, Scientific and Medical (ISM) bands which have frequency span, from 2.412 GHz to 2.482 GHz and from 5.15 GHz to 5.825 GHz [5]. Specifically, low-cost, simple to design solutions for antenna design are becomes critical and required since both the market and technology are so far ready for mass production [6]. Furthermore, network convergence and rapid diffusion of high-speed broadband has shifted attention towards broadband content. So the rapid high-speed broadband development, contemporary antenna systems demand, versatility unobtrusiveness, improved wireless security techniques, develops the need of the systems

that can perform over several frequency bands or a reconfigurable as the demands on the system changes and innovative use. This thesis presents the reconfigurable and broadband microstrip antenna for WLAN applications. It has been the goal of this research to design antennas that are not only discrete in design (low profile and compact) and can perform adequately (broadband and directive) but also circular polarized and reconfigurable.

1.2 PROBLEM STATEMENT

In recent years the constant evolution of technology has brought many previously unpopular innovations into the spotlight. One such technology now in the spotlight is cellular phones. Previously uncommon in modern society they are now widely used and accepted. Cellular technology leads the push towards wireless technology. Wireless LANs and Personal Communication Systems (PCS) are two such wireless technologies based on IEEE 802.11 a/b/g standards that are gaining popularity. With the popularity of wireless systems increasing, the development of antennas for these systems is becoming more important. The antenna can be considered as the backbone to a wireless system. Narrow band antennas are not suitable due to their limited bandwidth, and so the necessity is for broadband antennas. Antennas such as disc ones display highly broadband behavior but remain undesirable due to their aesthetic failings and lack of directionality. Microstrip antennas are extremely suitable for these applications; they are compact and low profile while offering good performance. The first stage of the thesis is to examine the various options available when designing and manufacturing microstrip antennas. The research will include investigations into the basic theory of microstrip patch antennas, matching techniques and broadbanding techniques. The second stage will

be to develop a couple of working prototype antenna designs and finally design a reconfigurable antenna that can perform over several frequency bands or to be reconfigurable as the demands on the system changes and innovative use.

1.3 MOTIVATION AND APPLICATIONS

1.3.1 MICROSTRIP ANTENNA: A LOW COST SOLUTION

Wireless communication has been developed rapidly in the past decade and it has already had a dramatic impact in our lives. In the last few years, the development of wireless local area networks (WLAN) represented one of the principal interests in the information and communications field. WLAN takes advantage of a license free frequency bands, Industrial, Scientific and Medical (ISM). Furthermore, for many Internet Service Providers (ISPs) it looks convenient to apply 802.11 based point-to-point links in order to provide the wireless coverage of the last mile towards the client. Thus, specific antenna systems are recently being developed to comply with requirements dictated by such applications. Specifically, low-cost, simple to design solutions for antenna design are becoming critical and required since both market and technology are so far ready to mass production [6]. However, the microstrip antenna has a limitation which is the narrow bandwidth of the basic element. The bandwidth of the basic patch antenna is usually 1 – 3%.

1.3.2 VERSATILITY OF MICROSTRIP ANTENNA

A WLAN antenna needs to be versatile and perform without prior alignment in order to reach the optimum throughput. With a circularly polarized wave, the receiving antenna

does not require to be configured and will pick up the signal for different orientations. This attribute of the antennas will be ideal for WLAN applications.

1.3.3 MULTIPLE FUNCTIONALITY OF MICROSTRIP ANTENNA

Antennas that can be used for multiple purposes, function over several frequency bands and can be integrated on a package for mass-production are the ultimate goals of commercial and defense investigators. Furthermore, applications of such systems in personal and satellite communications impose the requirement for elements miniaturized in size and weight. Reconfigurable antennas have recently received significant attention for their applications in communications, electronic surveillance and countermeasures, by adapting their properties to achieve selectivity in frequency, bandwidth, polarization and gain. Compared to broad band antennas, reconfigurable antennas offer the advantages of compact size, and similar radiation pattern for all designed frequency bands. Reconfigurable antennas have recently received significant attention for their applications in communications, electronic surveillance and countermeasures, by adapting their properties to achieve selectivity in frequency, bandwidth, polarization and gain. Compared to broad band antennas, reconfigurable antennas offer the advantages of compact size, similar radiation pattern for all designed frequency bands, efficient use of electromagnetic spectrum and frequency selectivity useful for reducing the adverse effects of co-site interference and jamming [7-11].

1.3.4 RECONFIGURABLE FREQUENCY FEATURE OF MICROSTIP ANTENNA

Dual frequency reconfigurable microstrip antennas can offer additional advantages of frequency reuse for doubling the system capability and polarization diversity for good performance of reception and transmission or to integrate the receiving and transmitting functions into one antenna for reducing the antenna size.

1.4 OBJECTIVES AND PROBLEMS / LIMITATIONS

The reduced size, dual band, reconfigurable antenna together with gain and bandwidth enhancement is the major objective of the thesis

1.4.1 BASIC ASSUMPTION AND LIMITATIONS

Common limitations of microstrip antennas are:

- Narrow bandwidth and associated tolerance problems.
- Relatively lower gain.
- Large ohmic loss in the feed structure of arrays .
- Most microstrip antenna radiate into half-space.
- Complex feed structures required for high-performance arrays.
- Polarization purity is difficult to achieve.
- Poor end-fire radiator, except tapered slot antennas.
- Extraneous radiation from feeds and junctions.
- Low power handling capability.
- Reduced gain and efficiency as well as unacceptably high levels of cross-polarization and mutual coupling within an array environment at high frequencies.

- Excitation of surface waves.

Microstrip antennas fabricated on a substrate with a high dielectric constant are strongly preferred for easy integration with MMIC RF front-end circuitry. However dielectric constant substrate leads to poor efficiency and narrow bandwidth.

The thesis presents some ways to minimize the effect of some of these limitations. For example, bandwidth enhancement by using a multiple resonance technique, dual band operation by using slits, directive and high gain by using a thin substrate with a low dielectric constant, circular polarization by using dual feeding, ease of fabrication because of simple design and reconfigurable in order to meet the recent demands of the wireless communications.

1.5 DOCUMENT OVERVIEW

The outline of this thesis is organized as follows:

Chapter 2 provides research background, recent trends, and the contribution of the thesis.

Chapter 3 provides a brief technical description of microstrip antennas focusing on broadband techniques, basic characteristics and typical excitation (feeding) methods, and concludes with an analytical model of a patch and an overview of the antenna design methodology.

Chapters 4 describes basic designs using rectangular, circular and triangular patch antennas.

Chapter 5 describes a novel reconfigurable microstrip antenna all of those chapters also give numerical results, with the help of graphs and concludes with a brief summary of how the proposed antennas have been used in the development of thin substrate

microstrip antennas, and with the introduction of a novel approach to designing patch antennas.

Chapter 6 describes the conclusion and future work and summaries the results and discusses possible applications.

CHAPTER II – LITERATURE REVIEW

2.1 INTRODUCTION

The increasing demand for cellular phone services, wireless internet access, wireless cable television, among others, force systems to provide high throughput, and therefore very large bandwidths as well as simultaneous access to different systems through the same device. This can be accomplished with multi-band or reconfigurable technology. But on the other hand there are two most serious limitations of the microstrip antennas its low gain and narrow bandwidth. The compact antenna configuration further degrades these two parameters. This is because of the fact that there is a fundamental relationship between the size, bandwidth and efficiency of an antenna. The gain is also related to the size of the antenna, that is electrically small antennas typically provide lower gain than larger antennas.

2.2 BASIC CHARACTERISTICS OF MICROSTIP ANTENNA (MSA)

As shown in Fig 2.1, conventional microstrip antennas consist of a pair of parallel conducting layers separating a dielectric medium, referred to as the substrate. In this configuration, the upper conducting layer or patch is the source of radiation where electromagnetic energy fringes off the edges of the patch and into the substrate. The lower conducting layer acts as a perfectly reflecting ground plane, bouncing energy back through the substrate and into free space. Although similar in operation to a microstrip transmission line, the patch antenna is much larger in volume providing a distinct contrast between the two. Physically, the patch is a thin conductor that is an appreciable fraction of a wavelength in extent, parallel to a ground plane and a small fraction of a wavelength

above the ground plane [12]. In most practical applications, patch antennas are rectangular or circular in shape [13]; however, in general, any geometry is possible.

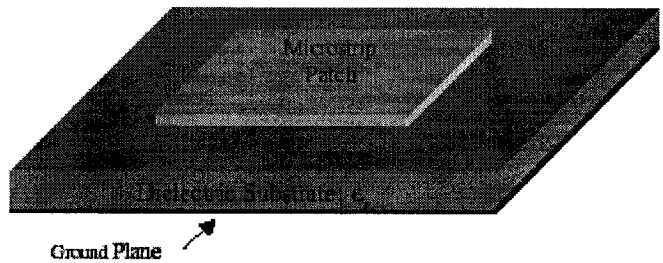

Figure 2.1 Typical geometry of a microstrip antenna.

2.3 MICROSTRIP ANTENNA CONFIGURATION

Microstrip antennas are different from many conventional microwave antennas. They are characterized by a greater number of physical parameters. They come in various geometrical shapes and dimensions. Microstrip antennas are classified into four basic groups namely microstrip patch antennas, microstrip dipole antennas, printed slot antennas and microstrip traveling-wave antennas, but the main focus of the thesis is on microstrip patch antenna .

2.3.1 GEOMETRICAL SHAPES OF MICROSTRIP ANTENNAS

A microstrip patch antenna (MPA) consists of a conducting patch of any planar or nonplanar geometry on one side of a dielectric substrate with a ground plane on the other side [32]. The basic rectangular microstrip patch antenna is shown in Fig 2.2. The most commonly used patch antennas are rectangular and circular patch antennas. A patch antenna exhibits a gain between 5 to 6 dB and has a 3-dB beamwidth between 70° and 90°.

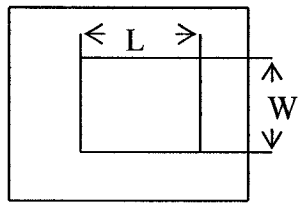

Figure 2.2 Rectangular microstrip patch antenna.

The radiating patch comes in various shapes like:

- Square.
- Rectangle.
- Triangle.
- Circle.
- Ellipse.
- Ring.

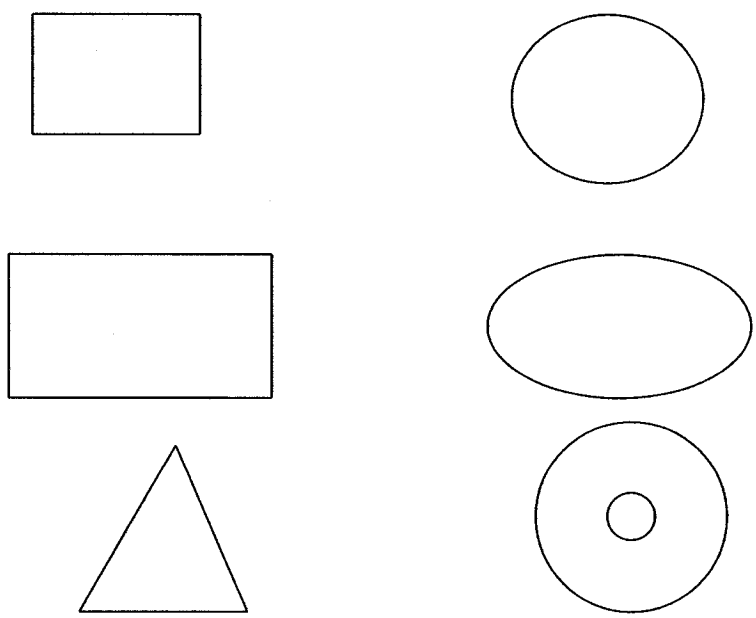

Figure 2.3 Basic microstrip patch antennas.

The most common and frequently used shapes are square, rectangular, triangular and circular as shown in Fig 2.3, because of their ease of analysis and fabrication, and their attractive radiation characteristics. They possess low cross-polarization radiation too. Microstrip dipoles are chosen quite often as they inherently possess a large bandwidth and occupy less space, which makes them suitable for arrays. Linear and circular polarizations can be achieved with either single elements or arrays of microstrip antennas. Arrays of microstrip elements, with single or multiple feeds, may also be used to introduce scanning capabilities and achieve greater directivities [12].

Commercial substrate materials are readily available for use at RF and microwave frequencies, specifically for the design of microstrip antennas and printed circuits. Selection is based on desired material characteristics for optimal performance over specific frequency ranges. Common manufacturer specifications include dielectric constant, dissipation factor (loss tangent), thickness, and Young's modulus. The range of dielectric constant is from $2.2 \leq \varepsilon_r \leq 12$ for operation at frequencies ranging from 1 to 100 GHz [12]. The thickness of the substrate is of considerable importance when designing microstrip antennas. The most desirable substrates for antenna performance are the ones that are thick with a low dielectric constant. This tends to result in an antenna with a large bandwidth and high efficiency due to the loosely bound fringing fields that emanate from the patch and propagate into the substrate. However, this comes at the expense of a large volume antenna and an increased probability of surface wave formation. On the other hand, thin substrates with high dielectric constants reduce the overall size of the [12] antenna and are compatible with MMIC devices, since the

fringing fields are tightly bound to the substrate. With thin substrates, coupling and electromagnetic interference (EMI) issues are less probable. However, because of the relatively higher loss tangents (dissipation factors), they are less efficient and have relatively smaller bandwidths [12].Therefore, there is a fundamental tradeoff that must be evaluated in the initial stages of the microstrip antenna design - to obtain loosely bound fields to radiate into free space while keeping the fields tightly bound for the feeding circuitry and to avoid EMI.

2.4 MICROSTRIP ANTENNA FEEDS

There are several techniques available to feed or transmit electromagnetic energy to a microstrip antenna. The most popular methods are the microstrip transmission line, coaxial probe, aperture coupling, and proximity coupling [13, 14]. The more popular feed networks are summarized below.

2.4.1 MICROSTRIP LINE FEED

The simplest way to feed a microstrip patch is to connect a microstrip line directly to the edge of the patch. In this case both the patch and lines are located on the same substrate. The matching between the characteristic impedance of the microstrip feed line and the patch can be done by selecting the right depth of the inset as shown in Fig. 2.4. [15]. A microstrip structure with the line and patch on the same level cannot be optimized simultaneously as an antenna or as a transmission line because the specific requirements for both are contradictory. A low dielectric constant is needed for the efficient radiation from the patch. However, it will result in spurious radiation from line and the step discontinuities.

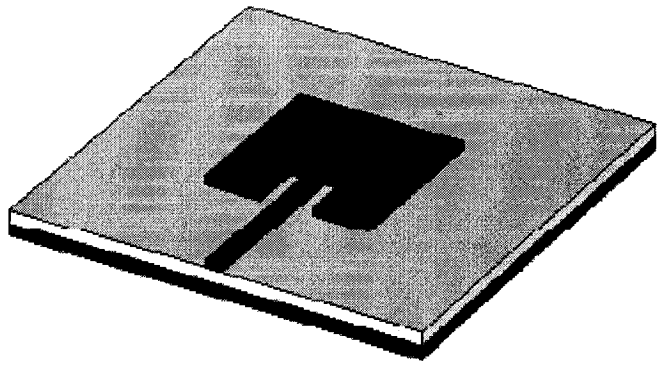

Figure 2.4. Patch antenna with microstrip line feed

This spurious radiation increases both the sidelobe level and the cross-polarization. The patch behaves like a cavity due to the accumulated reactive power below it. To reduce the radiation from the microstrip line if we use high dielectric constant substrate, it will degrade the radiation efficiency of the patch and increase the surface wave loss.

2.4.2 COAXIAL FEED

The coaxial feed is the simplest feed structure for the microstrip antennas and remains among the most popular one. It is a quite different way to feed a patch by means of a coaxial line that is set perpendicular to the ground plane as shown in Fig. 2.5. In this case the inner conductor of the coaxial line is attached to the radiating patch while the outer conductor is connected to the ground plane. The input impedance depends on the position of the feed so that the patch can be matched to the coaxial line by properly positioning the feed. It has low spurious radiation because the radiating and feeding systems are disposed on the two sides of the ground plane and shielded from each other. However, it is not suitable for antenna array applications [13-15].

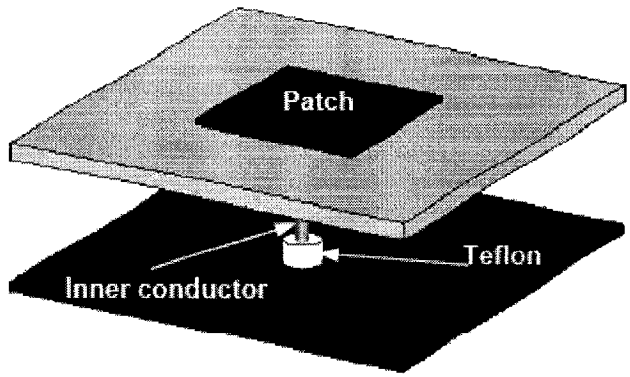

Figure 2.5 Patch antenna with coaxial line feed.

2.4.3 PROXIMITY COUPLING

Proximity coupling of the patch to the feed line is obtained by placing the patch and the feed at different levels as shown in Fig. 2.6. Using this feed, the frequency bandwidth of the patch resonator could be significantly widened (around 13%) and it gives low spurious radiation [15]. Using a thin substrate of high relative permittivity can considerably reduce the radiation from the feed. The upper dielectric layer is thicker and has a low relative permittivity, so that the radiation of the patch is enhanced. However, the feed line is no longer located on an open surface, so there is no direct access to it and one can not easily connect components within the feeding circuit.

2.4.4 APERTURE COUPLING FEED

The further step is to achieve the complete separation of the radiation and guided transmission functions. This separation can be achieved by placing the ground plane between the radiating patch and the feed system as shown in Fig. 2.7 [13-15]. Coupling between the microstrip feed line and the radiating patch is provided by a slot (aperture) in

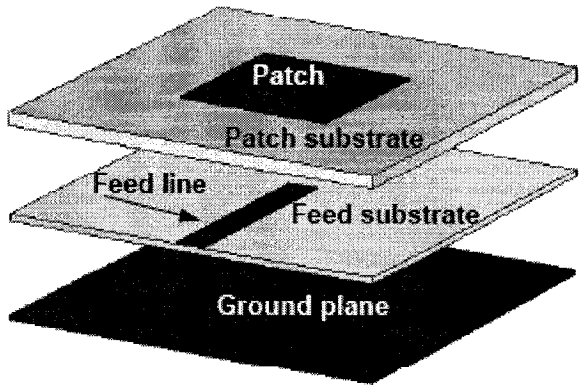

Figure 2.6 Patch antenna with proximity coupling feed.

the ground plane between the radiating patch and the feed system as shown in Fig. 2.7. Coupling between the microstrip feed line and the radiating patch is provided by a slot (aperture) in the ground plane. Radiation from the open end feed line does not interfere with the radiation pattern of the patch because of the shielding effect of the ground plane. Possible radiation from the feed line can be completely avoided by enclosing the bottom part within a shielded enclosure. The aperture coupling is not so simple to fabricate. The aperture coupling feed method has the advantages that one can easily integrate active components in the feed structure.

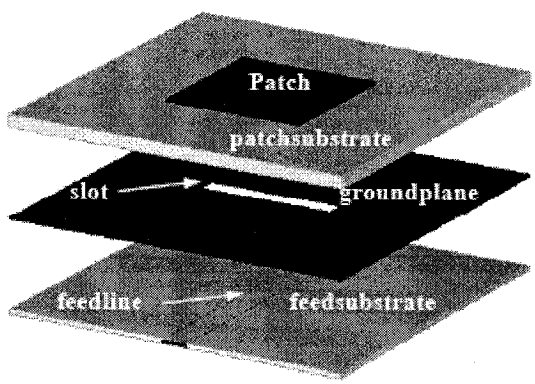

Figure 2.7 Exploded view of aperture coupling feed.

In both non-contacting configurations, there is an undesirable increase in the overall thickness of the antenna. Therefore, to reduce the complexity and size of the antennas involved in this research, it is decided to design the structures on a thin-low dielectric constant substrate i.e RT Duroid in all the proposed design, using a coaxial probe feed.

2.5 BROADBAND MICROSTRIP ANTENNA TECHNIQUES

A number of techniques have been reported by researchers to enhance the gain and bandwidth of microstrip antennas. Some of them used to enhance the gain are, loading of high permittivity dielectric substrate [16], inclusion of an amplifier type active circuitry [17] and stacked configuration [18]. Use of substrate loading technique helps in increasing the radiation efficiency. Amplifier circuits can also be integrated with the radiating patch to give rise to an active integrated antenna. In a stacked configuration, two patches, driven and parasitic, are used with the desired feeding technique. The narrow impedance bandwidth of the basic microstrip element is ultimately a consequence of its electrically thin ground-plane-backed dielectric substrate, which leads to a high Q resonance behavior. Bandwidth improves as the substrate thickness is increased, or the dielectric constant is reduced, but these trends are limited by an inductive impedance offset that increases with thickness. A logical approach, therefore, is to use a thick substrate or replacing the substrate by air or thick foam [19] with some type of additional impedance matching to cancel this inductance. A thick substrate introduces surface wave excitation. Another method reported [20] for the bandwidth enhancement is by loading the suspended microstrip antenna with a dielectric resonator. Besides impedance matching, another very popular bandwidth extension technique involves the use of two or more stagger tuned resonators, implemented with stacked patches, parasitic patches, or a

combination of dissimilar elements. Three dimensional patches like V-shaped patch [21], or wedge -shaped patch [22] can also be used to enhance bandwidth. Various feeding methods other than co-axial feeding, also enhances the bandwidth. Other reported methods use proximity feed [23], L-probe/ L-strip and Z-shaped feed [24]. The patch loaded with slots like U-slotted Patch, E- Patch [25], parasitic patches aside or on the top [26] also have effect on bandwidth enhancement. The stacked patch arrangement [27] is very popular, with reported bandwidths ranging from 10% to 20%. In this thesis, single-layered microstrip patch antenna on a relatively thin substrate are presented, which is based on multiple resonances without significantly enlarging the size.

2.6 BASIC PRINCIPLES OF BROADBAND DESIGN

The fundamental and basic principles of broadband design of microstrip and printed antennas are often discussed in the related papers and reports which are quite general and incomplete in true sense. References 1-6 cover this in a more detail. The basic principles are sometimes achieved using some other principles, which are in the phase of very rapid development. Thorough discussions are beyond the scope of this thesis and hence the main points are highlighted. The basic principles and their corresponding antenna geometries can be listed as:

1. Low Q-factor of the magnetic wall	Low dielectric constant or wall cavity under the patch larger thickness of the substrate
2. Multiple resonances	Parasitic patches in stacked or planar geometry, Reactive loading by shaped slot, notch, cuts, pin or post.
3. Impedance matching of the feed	Probe compensation using series capacitor, L-shape probe or any reactive loading
4. Optimization of patch geometry	Very irregular and unconventional patch shape optimized using Genetic Algorithm.
5. Suppression of surface waves	Periodic patterns on the ground plane or in a thick substrate: on any substrate produces Photonic Band Gap (PBG) Structure on one face of which microstrip element or arrays are printed.
6. Frequency dependent substrate	Multiple layers of Frequency Selective or ground plane: Surfaces (FSS) can reflect at respective frequency bands. For closely spaced frequency bands, the FSS combination acts over a larger frequency range as a pass band
7. Various combinations of (ii) and (iii).	

The recent trends in improving the impedance bandwidth of microstrip antennas can be broadly divided into the following categories:

- Various geometries and perturbations to introduce multiple resonances as well as input impedance matching.
- Genetic Algorithm (GA) based optimization of antenna geometries.
- Photonic Band Gap (PBG) structures used as printed antenna substrates.
- Frequency Selective Surfaces (FSS) used as multilayered substrate or ground plane.

The first one is leading all four categories in numbers and varieties and this thesis also based upon it.

2.7 CIRCULARLY POLARIZED MICROSTRIP ANTENNA TECHNIQUES

A microstrip antenna is an example of a resonator-type antenna. It primarily radiates a linear polarization and is designed for single-mode operation that radiates mainly linear polarization. A patch must support orthogonal fields of equal amplitude and in-phase quadrature for generating a circular polarized radiation.

2.7.1 CIRCULARLY POLARIZED PATCH

A microstrip patch is one of the most widely used radiators for circular polarization generation. A single patch antenna can be made to radiate circular polarization if two orthogonal patch modes are simultaneously excited with equal amplitude and ±90° out of phase with the sign determining the sense of rotation. The first type is a dual-orthogonal feed, which employs an external power divider network. The other is a single-point feed

for which an external power divider is not required [28]. Fig 2.8 shows two types of feeding schemes which can accomplish circular polarization.

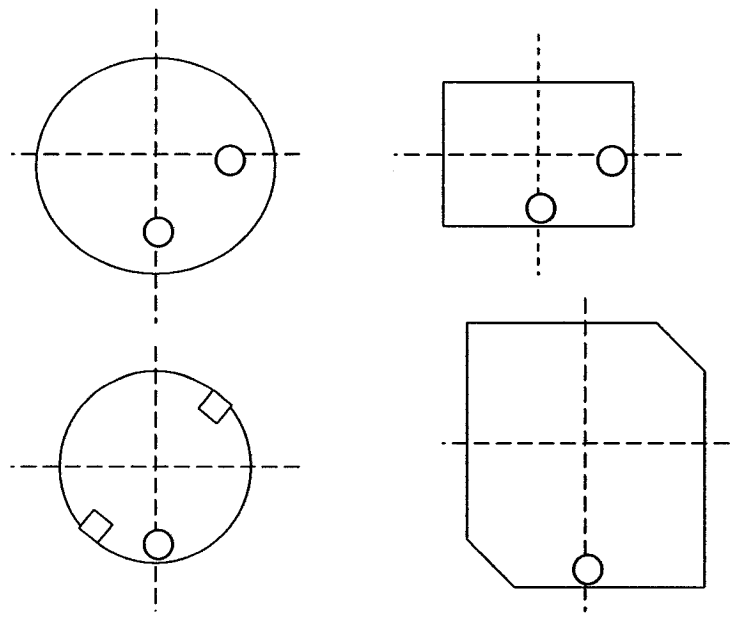

Figure 2.8: Two types of excitations for circularly polarized microstrip antennas.

2.7.2 DUAL-ORTHOGONAL FED CIRCULARLY POLARIZED PATCH

Figure 2.9 shows the configuration of a dual-orthogonal fed circularly polarized patch employing an external power divider. The shape of the patch is generally square or circular. The two orthogonal modes are excited by the dual-orthogonal feeds having equal amplitude but in phase quadrature. The power divider circuits that have been used for the generation of circular polarization are the quadrature hybrid, the ring hybrid, the Wilkinson power divider and the T-junction power splitter [29].

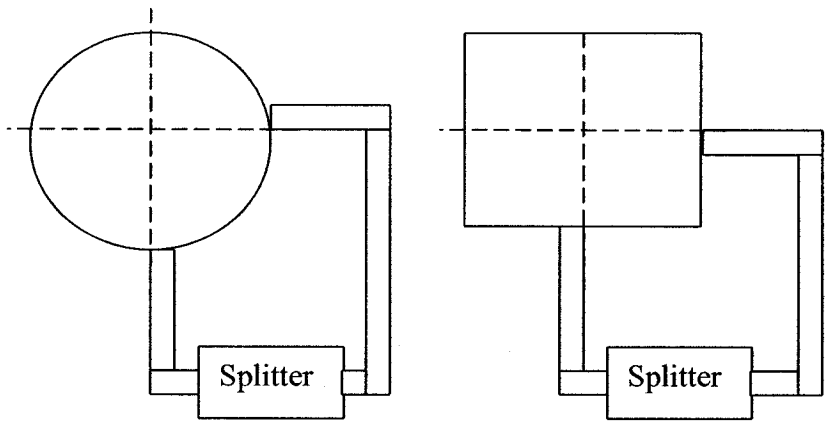

Figure 2.9: Configuration of dual-fed circularly polarized microstrip antennas.

2.7.3 SINGLY FED CIRCULARLY POLARIZED PATCH

Figure 2.10 shows the configuration of the singly-fed circularly polarized microstrip antennas. When it is not easy to employ dual-orthogonal feeds with a power divider network a single-point feed patch is employed in such case to produce circular polarization. In order to exhibit circular polarization it is essential for two orthogonal patch modes with equal amplitude and in-phase quadrature to be induced because a patch with a single-point feed generally radiates linear polarization. The slight perturbation of the patch at appropriate locations with respect to the feed accomplishes this task [28].

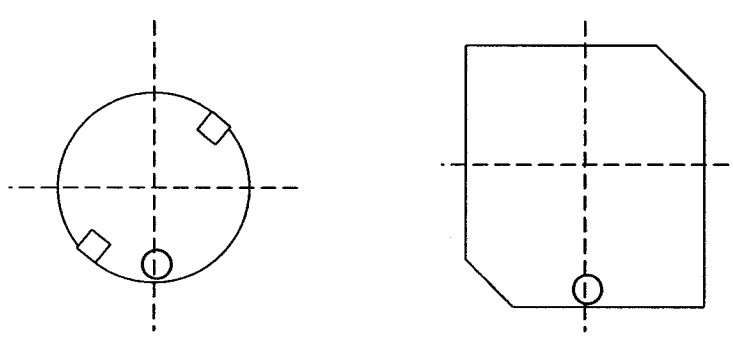

Figure 2.10: Configuration of singly-fed circularly polarized microstrip antennas.

2.7.4 SQUARE-TYPE CIRCULARLY POLARIZED MICROSTRIP ANTENNA

Figure 2.11 shows the different types of perturbations done in the singly-fed square type microstrip antenna for generating circular polarization [30]. The feed location is a very important criterion in this case. The feed is generally placed diagonal to the perturbation segments which are suitably selected to obtain two orthogonally degenerate modes in the patch for circularly polarized radiation.

Figure 2.12 shows the fundamental configuration of the patch and its coordinate system. The square patch is considered to be an electrically thin cavity with perfect magnetic walls at the boundaries, $x = \pm a/2$ and $y = \pm a/2$. In the figure 2.13, F is the feed point and ΔS represents the total sum of perturbation segments and may consist of a single or multiple segments [31].

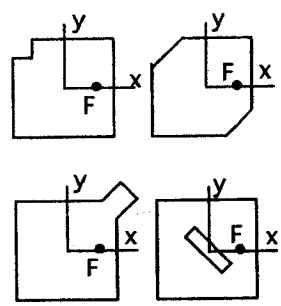

Figure 2.11: Different types of microstrip antenna perturbations for circular polarization generation.

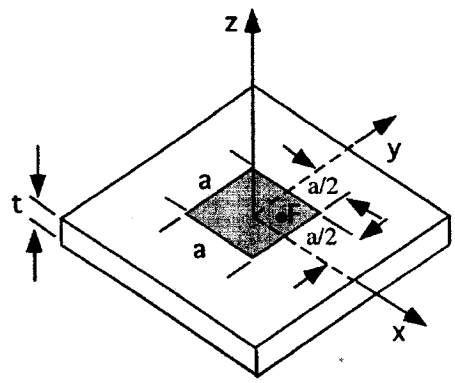

Figure 2.12: The fundamental configuration of the patch and its coordinate system. [28]

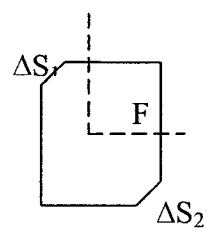

Figure 2.13: Microstrip patch antenna perturbations.

2.8 RECONFIGURABLE MICROSTRIP ANTENNA

Future generations of portable communication devices will require high quality wireless links capable of high data rate delivery, as well as the ability to maintain these links in harsh conditions or when communicating with multiple targets. To accomplish this, the use of innovative reconfigurable antenna designs should be considered to sustain the highest quality path for data. When the candidate antenna utilizes both reconfigurable radiation characteristics as well as frequency agility, the performance issues surrounding the integration, packaging and electromagnetic environment of the antenna become increasingly important factors and currently this is the main topic of many researchers who are trying to develop a process that can expediently predict the conditions for which

an antenna capable of altering its radiation and/or frequency characteristics can maintain a maximum degree of reconfigurability once integrated onto a host device.

Apparently the need for a reconfigurable radiation pattern antenna and a multifrequency antenna is obvious. An antenna design with a combination of those two reconfigurability characteristics would be highly desired. This research focuses on a technique to design a broadband, circularly polarized, and multiband patch antenna which at the same time maintains a multi frequency operation in a single low profile, low cost antenna.

CHAPTER III – THEORY AND DESIGN TECHNIQUES OF BROADBAND MICROSTRIP ANTENNA

3.1 INTRODUCTION

This chapter explains design technique, numerical and analytical model of broadband microstrip patch antennas. The chapter also explains the approximate and the accurate method of calculating different parameters of microstrip antennas. CAD microstrip antenna models are very complex, thus, no analytical expressions could be used and numerical methods should be used instead to approach the physical behavior of these devices. All these models resolve Maxwell's equations taking into account specific boundary conditions on the electromagnetic (EM) field. On the other hand, several numerical methods can be used for the rigorous characterization of these structures. All of these methods fall into three categories, namely,

- Integral methods (e.g. Moments Method).
- Differential methods (e.g. Finite Differences).
- Hybrid methods (combination of the two former methods).

The choice of any method of these should be based on several technical considerations such as the complexity degree of the studied structures and the nature of the boundary problem they present (i.e. scattering, radiation, propagation, etc.). Thus, for instance, differential methods such as FDTD and Finite Elements methods are very suitable for scattering and radiation problems while the integral methods, such as the Galerkin and the LSBR methods, are well suited for the propagation problems in closed structures. However, "personalized" methods (Hybrid methods), that combine two or more different methods in order to optimize the numerical performances of the obtained method, could

be used for the rigorous analysis of transmission structures involving regions of a smooth geometry and others of a complex one. Hence, for the first kind of regions an integral method can be used while a differential method that would allow a deep insight into the geometrical details of the latter regions should be used.

3.1.1 ANALYTICAL MODEL AND TECHNIQUES

In common practice, microstrip antennas are evaluated using one of three synthesis methods: the transmission line model, the cavity model, or the full wave model [13]. The approximate, simple and easy analytical model is the cavity model. But more rigorous and accurate model is the full wave model, with help of which one can analyze several complex models with special geometries, complex substrates, and mutual coupling from neighboring elements in an array.

3.1.2 RADIATION MECHANISM OF A MICROSTRIP ANTENNA (CAVITY MODEL)

The energization of the microstrip patch antenna establishes distribution of charge on the upper and lower surfaces of the patch, along with the surface of the ground plane. This is shown in Fig 3.1 for a rectangular patch.

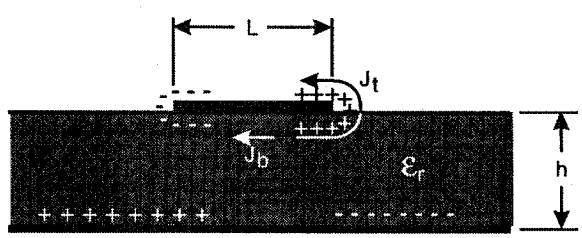

Figure 3.1 Current density and charge distribution on a microstrip antenna [29].

The -ve and +ve nature of the charge distribution arises because the patch is about a half-wave long at the dominant mode. The repulsive forces between like charges on the bottom surface of the patch tend to push some charges from the bottom surface, around its edges, to its top surface [29]. Fig 3.1 shows that the movement of charges creates corresponding current densities $\overrightarrow{J_b}$ and $\overrightarrow{J_t}$ at the lower and upper surfaces of the microstrip patch. The ratio h/w is very small for most microstrip antennas implying that the attractive force between the charges dominates. The majority of the charge concentration and the current flow are confined underneath the patch. A weak magnetic field exists which is tangential to the edges because a small amount of current flows encircling the edges of the patch to its top surface. We can assume that the tangential magnetic field is zero and magnetic walls can be placed around the circumference of the microstrip patch. Thin substrates with high ε_r confirms to this assumption. Also since the substrate used is very thin compared to the wavelength ($h << \lambda$) in the dielectric, the field variations along the height can be considered to be constant and the electric field nearly normal to the surface of the patch. Consequently, the patch can be modeled as a cavity with electric walls (because the electric field is near normal to the patch surface) at the top and below and four magnetic walls along the edges of the patch (because the tangential magnetic field is very weak) [29]. TM modes exist in this type of cavity. The dominant mode in this case is the TM_{100} mode and the electric field distribution is given in Fig 3.2.

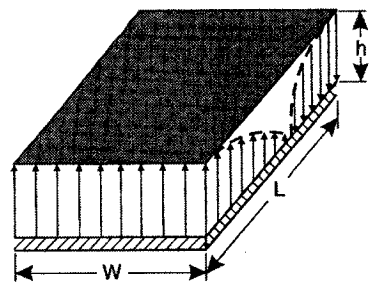

Figure 3.2 TM_{100} mode electric field distributions [29].

The four sidewalls of the cavity represent four narrow apertures or slots through which radiation takes place. Using the Huygen field equivalence principle, the microstrip patch can be represented by an equivalent current density $\overrightarrow{J_t}$ at the top surface to account for the presence of patch metallization. The four side slots are represented by the equivalent current densities $\overrightarrow{J_t}$ and $\overrightarrow{M_s}$ responding to the magnetic and electric fields $\overrightarrow{H_a}$ and $\overrightarrow{E_a}$ respectively in the slots [29].

The equivalent currents are given by

$$\overrightarrow{J_s} = nxH_a \tag{3.1}$$

$$\overrightarrow{M_s} = -nxE_a \tag{3.2}$$

The patch current present at the top $\overrightarrow{J_t}$ is much smaller than the current which is present at the bottom $\overrightarrow{J_b}$ for thin substrates. As there is negligible radiation from the patch current it is set to zero. The tangential magnetic fields present along the patch edges and current density due to it are also set to zero. Thus the only nonzero current density is the equivalent magnetic current density $\overrightarrow{M_s}$ along the periphery of the patch [29]. The radiation from the microstrip patch can be modeled with four ribbons of magnetic current radiating in free space.

The current density in this case is given by

$$\overrightarrow{M_s} = -2nxE_a \tag{3.3}$$

For the dominant mode the slot electric field $\overrightarrow{E_a}$ is given by

$$\overrightarrow{E_a} = z\overrightarrow{E_o} \tag{3.4}$$

for the slots of height h and length W. The other two slots of length L and height h

$$\overrightarrow{E_a} = -zE_o \sin(\frac{\pi x}{L}) \tag{3.5}$$

3.1.3 THE MOMENT METHOD

The Moment Method is a numerical method of solving integral equations (a sought function, e.g. current distribution on the antenna, is included in the integrand).

The method consists of the discretization of the analyzed structure, formal approximation of the sought function (known as basis functions and unknown approximation coefficients), substituting the formal approximation to the integral equation (unknown approximation coefficients are removed from the integral and the known basis functions are integrated), and minimizing the approximation error The solved equation containing the formal approximation is sequentially multiplied by Dirac pulses in the center of discretization elements and the product is integrated over the whole analyzed structure. We obtain N equations for N unknown approximation coefficients) and in solving the final matrix equation (unknown approximation coefficients, and therefore, the approximation of the solution is obtained). The method of moments is further described in Appendix B.

3.2 DESIGN METHODOLOGY

In order to reach the primary goal of manufacturing broadband patch antennas, the thesis is split into subtasks, which allowed for achievable short-term goals. After the initial research regarding microstrip antennas, specific work needed to be done as shown in the flow chart Fig 3.6.

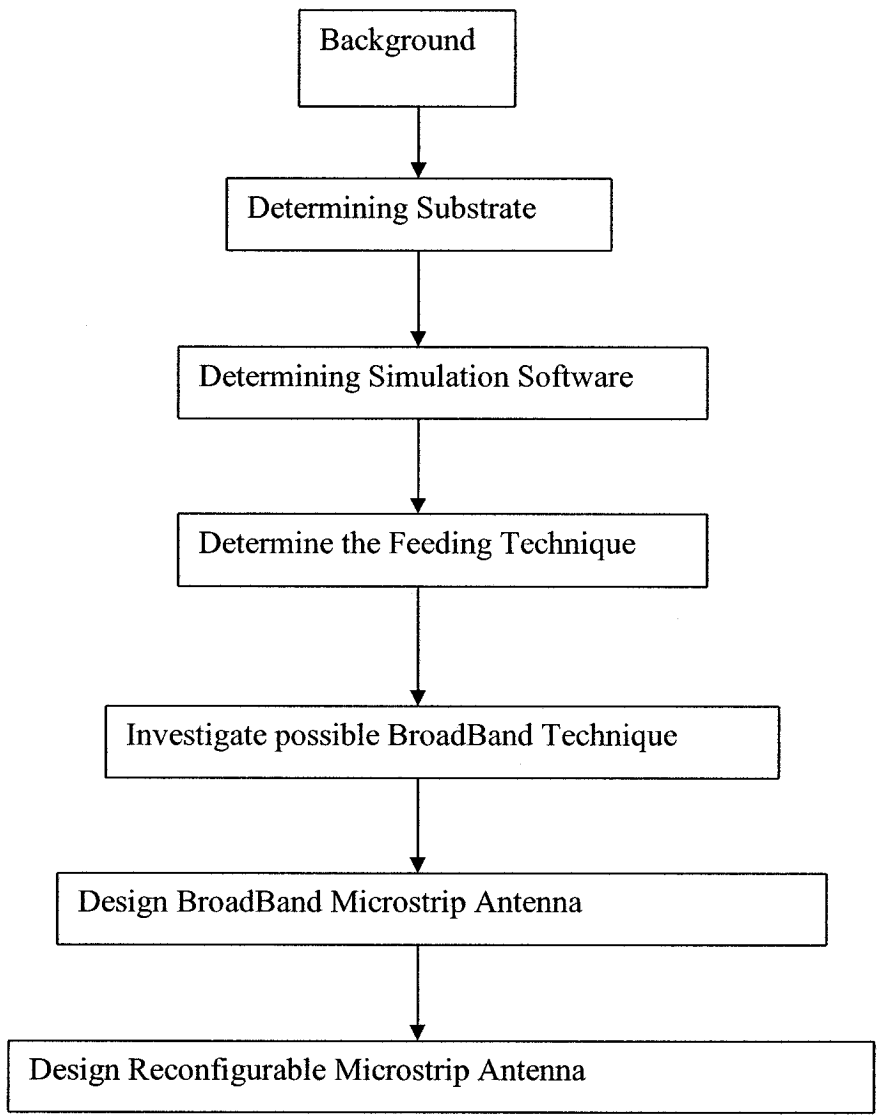

Figure 3.6 Design methodology.

3.2.1 PERMITTIVITY OF DIELECTRIC SUBSTRATE

Dielectric substrates should:

- Provide a stable mechanical support for the microstrip structure.
- Ensure that the components located on it are held firmly in place.
- Concentrate electromagnetic fields.
- Prevent unwanted radiation.

The choice of substrate material is governed primarily by two parameters – its dielectric constant (permittivity) and its height (or thickness). Of course, other aspects, such as cost, mechanical rigidity, conductivity etc., will also have to be considered. Table 3.1 shows the characteristics (permittivity and thickness) of broadband patch antennas

Application	Thickness	Permitivity
Antenna (Radiating)	Thick	Low
Antenna (Non-radiating)	Thin	High
Surface Waves (Unwanted)	Thick	High

Table 3.1 Desired substrate characteristics.

It is apparent from the Table 3.1 that the substrate characteristics needed for an antenna contradict those required for microstrip circuits or transmission lines. Thus, to achieve good performance for the two applications concurrently, different substrates with suitable attributes are essential. Concentration of electromagnetic fields near its conductor(s) can be achieved by mounting circuits upon electrically thin substrates with low permittivity. On the contrary, radiations of electromagnetic fields from antennas are best furnished by thick substrates with low permittivity. Thick substrates with high dielectric constants will promote unwanted surface waves. Surface waves have a threefold negative effect. Firstly, they dilute some of the signal energy thereby lowering power efficiency. Secondly, introduction of spurious coupling degrades circuit/transmission line performance due to interaction between elements. Lastly, surface waves terminating at circuit boundaries will reflect and/or diffract, which contributes to undesired radiation causing the ill-effect of increased sidelobe levels. So the best choice of the substrate chosen for this thesis is RT Duroid 5880, which is comparatively thin (62 mils) as compared to other broadband antennas.

3.2.2 APPLIED BROADBAND TECHNIQUE

Bandwidth enhancement by multiple resonances is a widely used technique for microstrip patch antennas. There are numerous methods to couple multiple resonances. Examples include coupled patches [33], patches with slots (e.g. U- and E-shaped) [32, 34], stacked patches [35], and patches with aperture-coupled feeds [36]. In some personal wireless communications systems, such as used for triple band option, more than 30 percent of the operating bandwidth is required. Bandwidth in excess of 70 percent can be achieved with aperture-coupled stacked patches. However, such configurations occupy considerable

space and are not always acceptable for integration with other circuitry. For handheld wireless systems, a compact single patch on moderately thick substrate is preferred. For such an antenna, achieving more than 25% bandwidth and moderate gain presents a challenge. The best scheme is chosen based on manufacturing simplicity without compromising performance over the frequency band concerned. Therefore, in this thesis, we present a single-layer microstrip patch antenna on a relatively thin substrate. The design employs multiple resonances without significantly enlarging the size. Three broadband patches are produced during this phase; using the same technique but using different shape and geometry. All three patches are thoroughly tested for bandwidth (BW) and tuned to best match the input impedance. Chapter 4 will show the field performance of all those different shape and the results. Figure 3.7 shows prototype designs of broad band patch antenna using multiple resonant techniques.

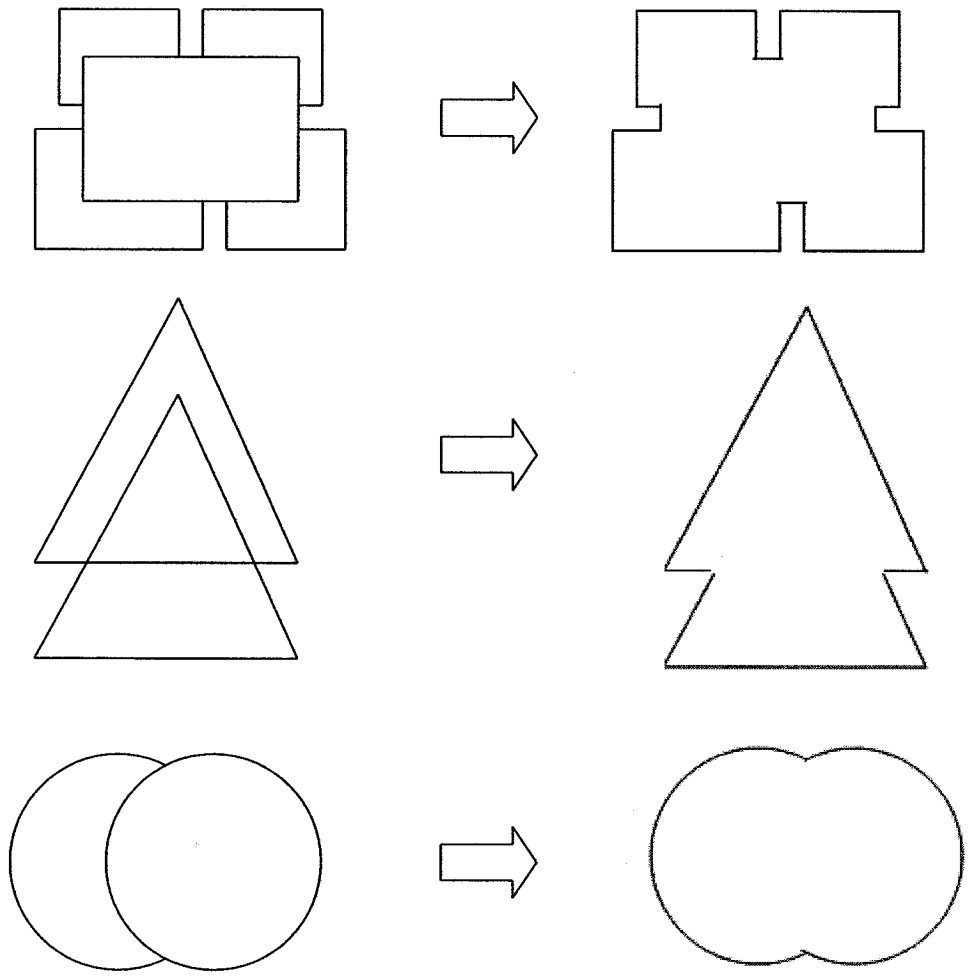

Figure 3.7 Prototype Designs using multiple resonant techniques

CHAPTER IV – BROAD MULTI-BAND CIRCULARLY POLARIZED MICROSTRIP ANTENNA

4.1 INTRODUCTION

The rectangular patch antenna is the basic and most commonly used microstrip antenna. These patches can be used for the simplest and most demanding applications. For example, characteristics such as dual and circular polarization, dual-frequency operation, frequency agility, broad bandwidth, feed line flexibility, beam scanning, omni directional patterning, and so on are easily obtained using this patch shape [12-13]. Because these geometries are separable in nature, their analysis is also relatively simple, this simplicity has led to their being the topic of a large number of research papers [1-11] that are too numerous to list. In this design, a new compact single-layer microstrip patch antenna has been proposed on a relatively thin substrate to achieve broad bandwidth of about 36.36% centered at 2.5 GHz. The proposed antenna is very suitable for IEEE 802.11x. To increase the bandwidths of the patch antenna, multiple resonances technique is used.

4.2 GEOMETRY

Five rectangular patches with three different dimensions (W1 x W2), (W3 x W4) and (W5 x W6) are overlapped as shown in Fig 4.1 respectively.

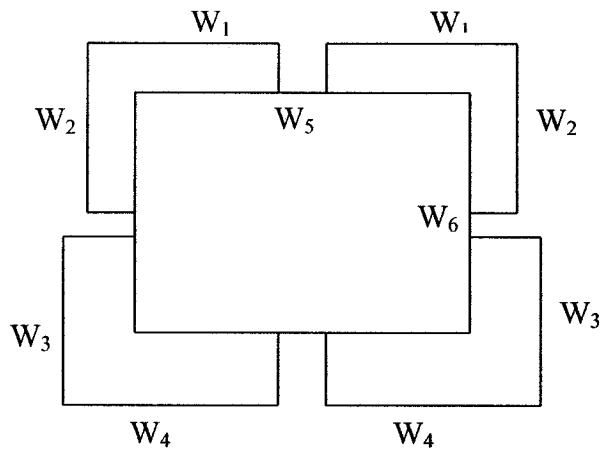

Figure 4.1 Multiple resonances using rectangular patches

According to Figs 4.1 and 4.2, the structure has 2 different resonant lengths as follows

$L1 = W1 + W1 + (2W1 - W5) + 2\Delta L_1$

$L1 = 4\,W1 - W5 + 2\Delta L_1$

$L2 = W4 + W4 + (2W4 - W5) + 2\Delta L_2$

$$L2 = 4W4 - W5 + 2\Delta L_2 \qquad (4.1)$$

The incremental lengths, ΔL_1, and ΔL_2 are due to the fringing fields and can be computed from

$$\Delta L_1 = \frac{0.412(\varepsilon_{eff} + 0.3)(20/h + 0.264)}{(\varepsilon_{eff} - 0.258)(20/h + 0.8)} \quad \Delta L_2 = \frac{0.412(\varepsilon_{eff} + 0.3)(18/h + 0.264)}{(\varepsilon_{eff} - 0.258)(18/h + 0.8)} \qquad (4.2)$$

Note that there are 18 parameters that may influence the performance of the proposed antenna: the length and width of four slits and five rectangles. Extensive simulations to study the effect of these parameters have been carried out but not included. The resonant length, based on (4.1) is kept constant and all other parameters have been optimized for a 10 dB wide bandwidth using simulations. Different frequency bands and results can be obtained by changing those parameters.

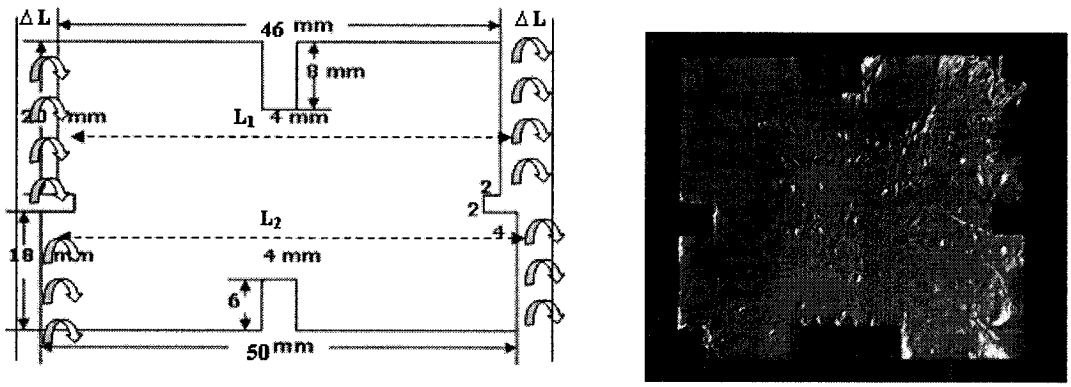

Figure 4.2 Geometry of the proposed antenna

Figure 4.2 shows how the field 'fringes' off the radiating edges of a rectangular patch. These fringing fields will affect the apparent electrical length of the patch, thereby altering its resonant frequency.

4.3 RESULTS AND DISCUSSION

The patch antenna is fed with two probes to operate over 2.45 GHz. The substrate used is RT Duroid 5880 with thickness of 1.575 mm and dielectric constant of 2.2. The patch antenna is centered at (0, 0).The feed points are located at (-26mm, -16mm) and (26mm, 16mm). The structure has two different resonant lengths, shown in Table 4.1. The resonant frequency and bandwidth are the first data point's measure for patch antennas. The antenna is designed on Ansoft Ensemble method of moment software. Multiple resonances technique have been obtained by overlapping five rectangular patches. To assure accuracy each segment size is maintained smaller than $\lambda/20$. To be on the safer side and avoid remeshing the geometry, the 1-6 GHZ band of frequency is used throughout the process. The simulated and measured results are shown in Fig 4.3.

Resonant length Calculated	**Physical Dimension (mm)**	**Fringing field length (mm)**	**Total Length (mm)**	**Resonance frequency (GHz)**
L_1	48	0.92	48.92	2.66
L_2	50	0.92	50.92	2.52

Table 4.1 Comparison of resonant frequencies.

The simulated and measured results are very close to the computed data shown in Table 4.1. At the 2.45 GHz operating frequency the antenna has two radiating strips L_1 and L_2 parallel to each other that helps to get the wider band of about 36.36 % (simulated) and 28.5% (measured). Also the center frequency downshift is observed. This down shift is due to the imperfect soldering at the corners, which reduces the electrical length of the patch. Also the discrepancy between the simulation and measurement results can be attributed to the finiteness of the ground plane, and the fact that the response of the system is very sensitive to the exact location of the microstrip probe feed which is subject to alignment errors in the implementation process.

In addition, the narrower bandwidth in measurements compared to the simulation result, might be due to the fabrication accuracy of the vertical-coupling overlap design that is optimized for the original resonant frequencies and not for the shifted frequencies.

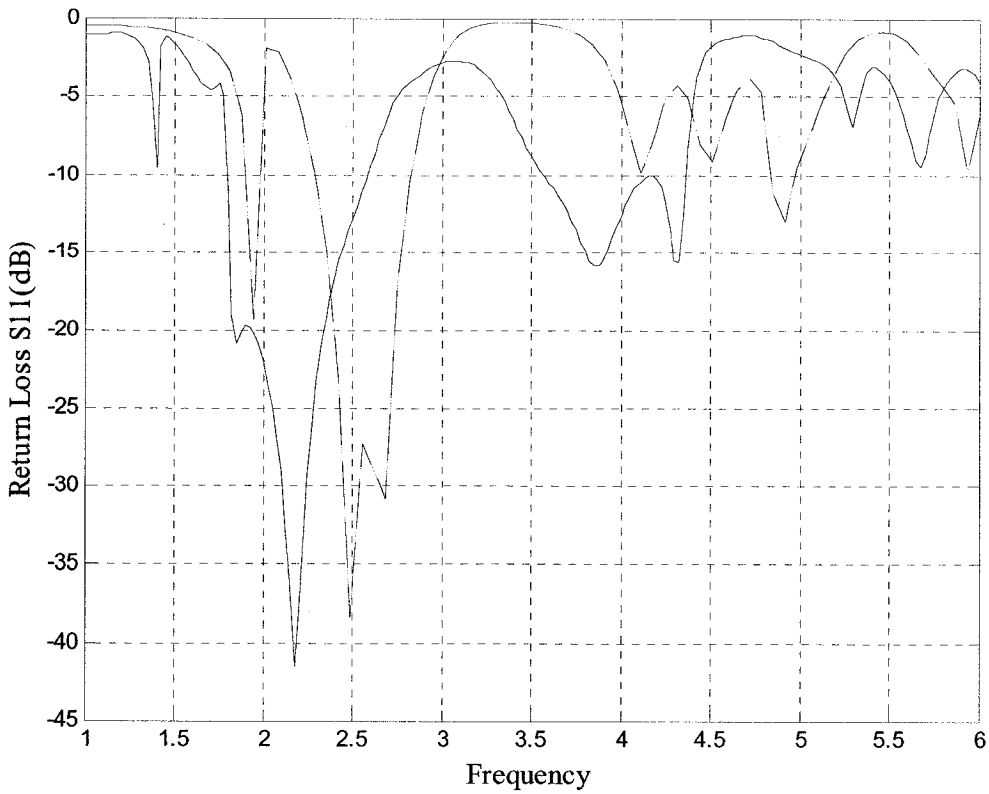

Figure 4.3 Return loss.

———	Simulated
- - - - -	Measured

4.3.1 RADIATION PATTERN MEASUREMENT

Once the resonant frequencies are identified, principal radiation patterns are taken to characterize the operational performance of each patch. These measurements are obtained using the indoor anechoic test chamber shown in Fig 4.4.

Principal radiation patterns consist of collinear polarization (co-pol) cross polarization (x-pol) plots, which are broken into either E-plane or H-plane cuts. The convention used in this thesis is that the orientation of the electric field line of the patch defines the E-plane. Likewise, the orientation of the magnetic field lines of the patch defines the H-

plane. For the patch designs, the electric field propagates along the XZ-plane of the patch and defines the E-plane cut, in a similar fashion; the YZ-plane defines the H-plane, which is perpendicular to the E-plane. The polarization of the pattern measurement, either collinear or cross, is defined by the polarization of the source antenna.

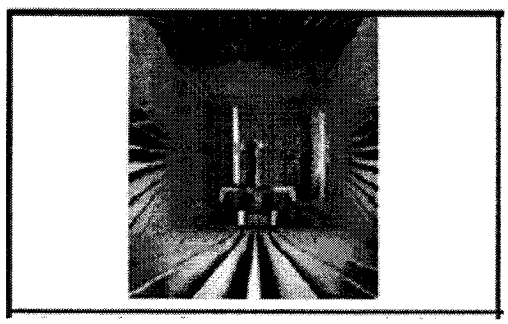

Figure 4.4 Image from the source antenna looking into the chamber and at the AUT.

With the proper antenna polarization, the principal antenna patterns are measured, as illustrated in Figs 4.5, 4.6 and 4.7 for the E-plane and H-plane co-pol respectively. As observed in the graphs, the direction of maximum radiation is located at boresight minus the angle in which the line of sight is the shortest.

Simulated

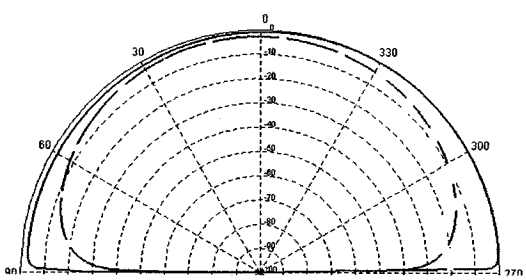

Measured

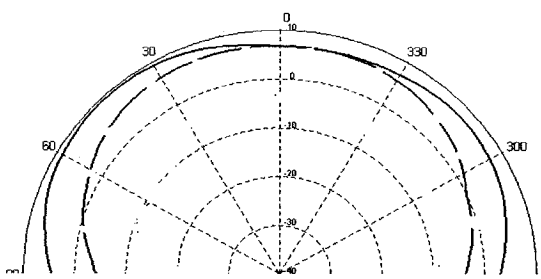

Figure 4.5 Comparison of the E-plane and H-plane antenna patterns at 2.3GHz.

Simulated Measured

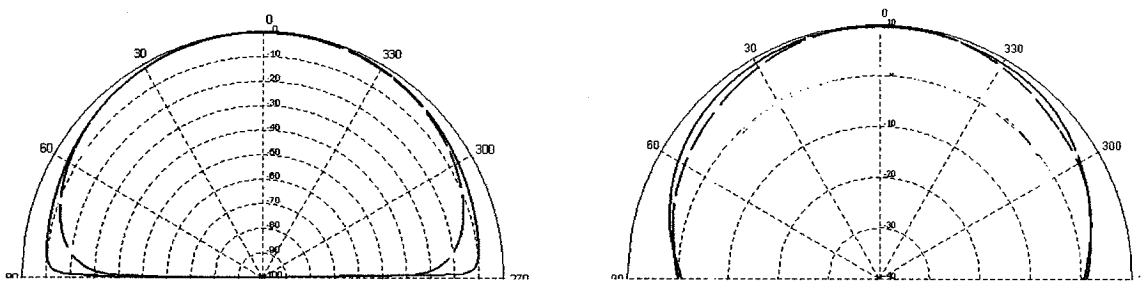

Figure 4.6 Comparison of the E-plane and H-plane antenna patterns at 2.5GHz.

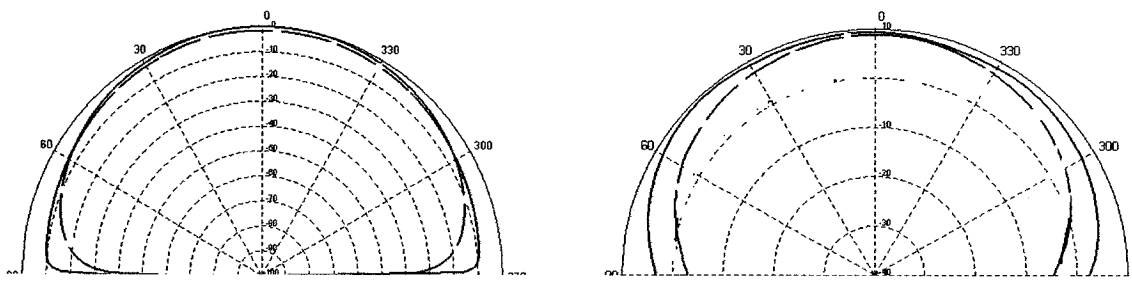

Figure 4.7 Comparison of the E-plane and H-plane antenna patterns at 2.8GHz.

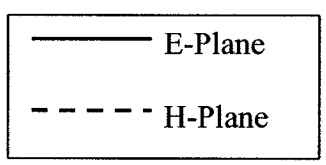

Despite the evident design error, there is still some valuable information obtainable from these measurements. First, an estimation of directivity is obtainable by evaluating the half power beamwidths (HPBW) of the principal radiation patterns. Using the co-pol radiation plots, the HPBW points are determined by locating the angle of maximum illumination and then locating the angles associated with an E-field intensity that is 3dB less or half-power. The result is that the patch at 2.8GHz antenna is more directive (D = 10 dB) than at 2.3GHz (D = 8.0 dB).

4.3.2 ADDITIONAL EXPLANATION OF RESULTS

To identify the behavior of the off-boresight antenna patterns detailed investigations on the design methodology are performed. The most suspicious parameter in the design is the placement of the feed. It is strongly believed that the probe offset during manufacturing the design resulted in the excitation of higher order modes and the beginning of circular polarization, which in turn resulted in an off-boresight radiation. This is a fundamental flaw in the design, in that the design is focused on establishing a perfect match between the antenna and feeds. Using this approach, pattern polarization and operating mode are ignored, leading to the apparent excitation of higher order modes and circular polarization. Upon further investigation, HFSS also verified that the patch is indeed operating in an undesired mode. Instead of operating in the dominant TM_{010} mode, the field from the patch radiate as if operating with a TM_{110} mode. This is determined by observing how the E-fields radiates on the surface of the patch. As illustrated in Fig 4.8, the field lines flow off the corners of the substrate oppose to the flat edges for radiation with in a TM_{010} mode. This field line orientation is a classical exhibition of a patch operating in a TM_{110} mode, which is favorable for circular polarization. This explains the unusually large x-pol pattern that is uncommon for linear polarized antennas.

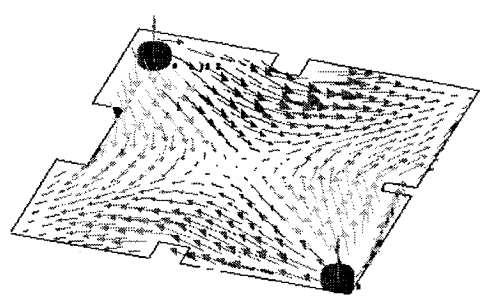

Figure 4.8 Illustration of the current vector.

4.4 CIRCULAR PATCH ANTENNA - INTRODUCTION

4.4.1 GEOMETRY

An antenna prototype has been designed at 5.4GHz, on a 1.57 mm height RT Duroid 5880 with relative permittivity 2.2, using Ansoft Ensemble simulation software [37]. The geometry of the design is very simple as shown in Fig 4.9. The design depends on two circular patches, of radius R, each which is equal to $\lambda /2\pi$. The center frequency chosen for this design is 5.5GHz. After numerous simulations the best result is found by combining two circles along the center in a way so that the distance between the two edges is equal to 3R, the feed points are located 1 mm above and below the axis on both the sides that helps to produce broadband operation. Different results can be obtained by changing the radius and the distance between two circular patches. To assure accuracy each segment size is maintained smaller than $\lambda/20$. To be on the safer side and avoid remeshing the geometry the 1-6 GHZ band of frequency is used throughout the process

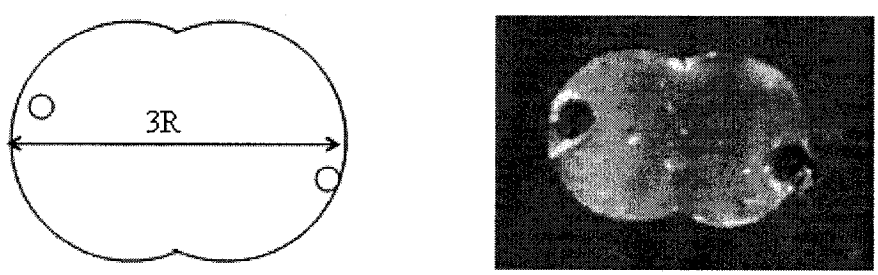

Figure 4.9 Geometry of the proposed design with R= 8.6 mm.

4.4.2 RETURN LOSS

The measurement and simulation results of input return loss are shown in Fig 4.10. The bandwidth from the measurement result is 19.86 % and the bandwidth using simulation result is 31.48%. There is a close agreement between the simulation and measurement

results for the bandwidth. The simulation results give a good approximation for the measurement even though the frequency has been shifted slightly from the simulation result.

There is a good resemblance between the two curves, but with a slightly poorer value of S11 for the prototype. The values are -25 dB and -23.5 dB respectively. One of the main reasons that the measured result is not as good as the simulated is probably a result of the not so perfect soldering of the contact on to the antenna. Also discrepancy between the simulation and measurement results can be attributed to the finiteness of the ground plane, which causes a shift in the resonance frequency and the fact that the response of the system is very sensitive to the exact location of the microstrip feed which is subject to alignment errors in the implementation process

4.4.3 RADIATION PATTERN AND AXIAL RATIO

Finally, to examine the radiation performance of the proposed antenna, patterns are measured inside an anechoic chamber. First, for comparison purpose, the simulated and measured radiation patterns in the E- and H-planes at 5 GHz, 5.5GHz and 6 GHz are presented in Figs 4.11, 4.12, and 4.13. The comparison between the simulated and measured results show a good agreement, validating the proposed design, and it can be noted that the proposed antenna has stable patterns across the operating band. The radiation pattern is in the broadside direction. The radiation pattern in both E and H-plane is omni directional. The co-polarized simulated radiation patterns are very similar to the measured radiation pattern, the measured cross-polarization (-12.5dB) at centre frequency is much better than the cross-polarization at side frequencies 5.0 and 6.0 GHz, respectively.

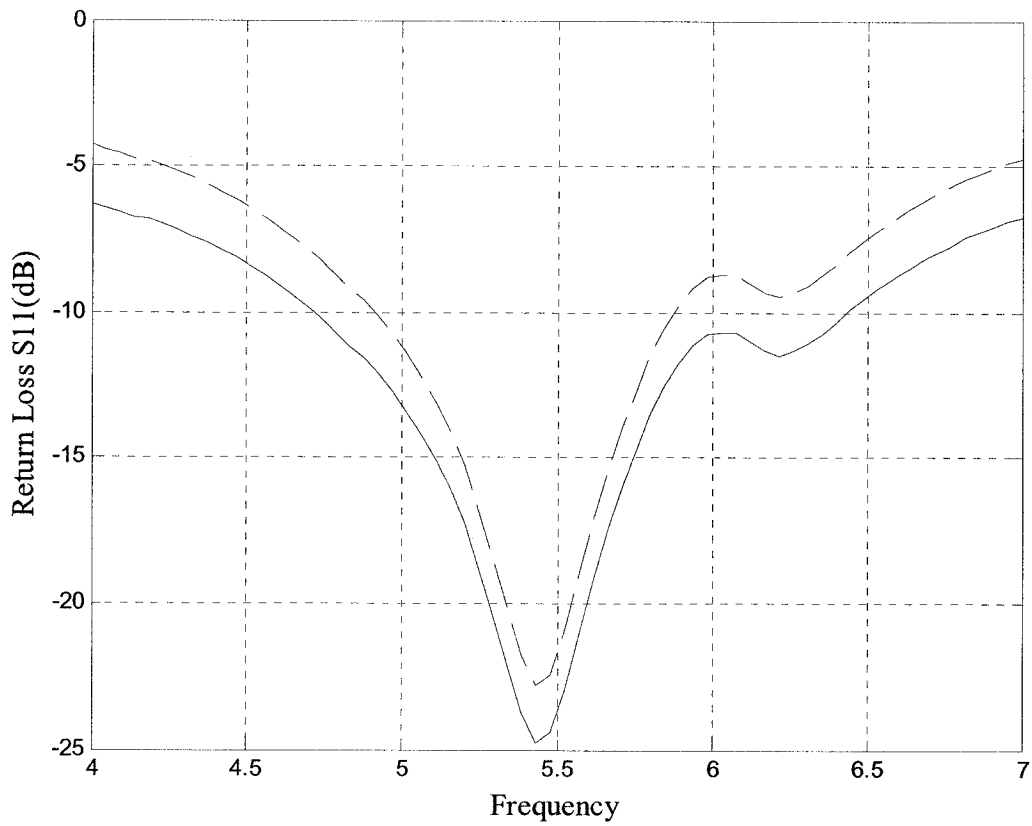

Figure 4.10 Return loss.

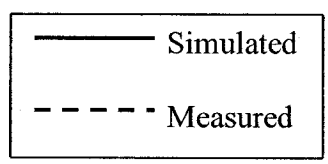

Simulated Measured

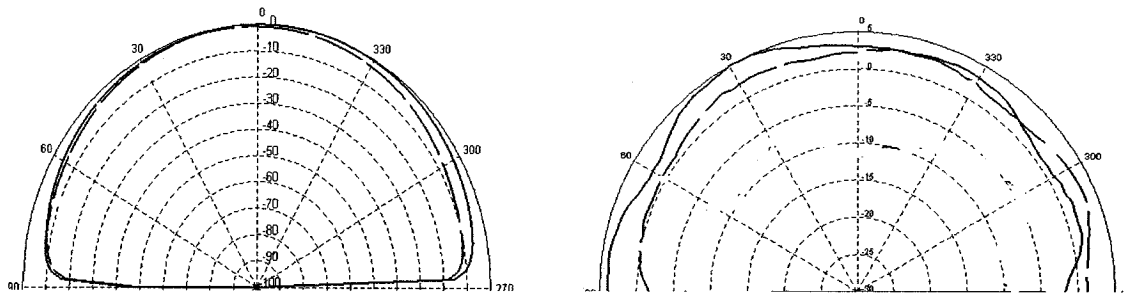

Figure 4.11 Comparison of the E-plane and H-plane antenna patterns at 5.5GHz.

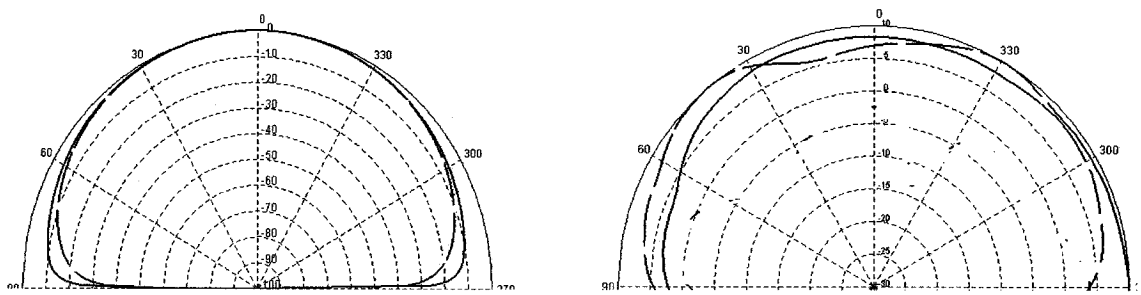

Figure 4.12 Comparison of the E-plane and H-plane antenna patterns at 5.0 GHz.

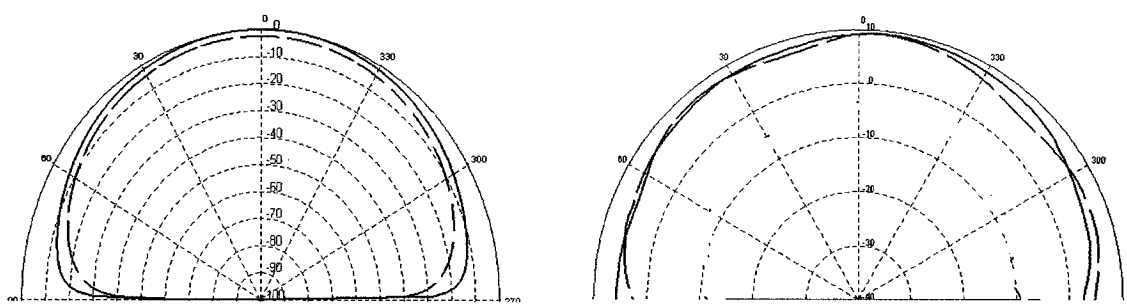

Figure 4-13 Comparison of the E-plane and H- antenna patterns at 6.0GHz.

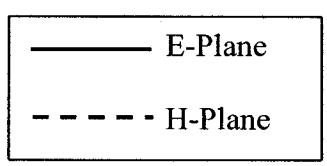

4.5 TRIANGULAR PATCH ANTENNA

4.5.1 GEOMETRY

The geometry of a two probes fed equiangular triangle patch antenna is shown in Fig 4.14. The technique to obtain a broader bandwidth is to take advantage of the resonant current distribution flowing on the antenna. The proposed antenna consists of two equilateral triangles patches with equal sides, 55 mm each, which can be calculated from the formula (A.32) given in Appendix A. After many simulations the best result is found by combining both patches along the centroid so that the distance from head to tail is 60 mm. Different results can be obtained by changing the length of equilateral triangles and the distance between them. The patch is centered over a dielectric RT Duroid 5880. The two probe feed patch antenna is designed to operated over the 2.1-2.6 GHz, 4.25GHz, 5.4GHz and 5.8GHz frequency bands. The antenna is simulated using Ansoft Ensemble method of moment software [37]. The return loss is shown in Figure 4.15. To assure accuracy each segment size is maintained smaller than $\lambda/20$.To be on the safer side and avoid remeshing the geometry the 1-6 GHZ band of frequencies is used throughout the process. The multiple resonances technique has been used by overlapping two equilateral triangles and it can be seen by observing the dip in the return loss rectangular patches.

4.6 RESULTS AND DISCUSSION

The bandwidth from the measurement result is 21.73 % and the bandwidth using simulation result is 28.28% for the 2.1-2.6 GHz band. The experimental result shows that the frequency has been shifted up by 300 MHz. This down shift is due to the imperfect soldering at the corners, which reduces the electrical length of the patch, which causes a

shift in the resonance frequency and the fact that the response of the system is very sensitive to the exact location of the microstrip feed which is subject to alignment errors in the implementation process

Although there is a little agreement between the simulation and measurement result for the bandwidth yet the simulation results give a good approximation for the measurement even though the frequency has been shifted slightly from the simulation result.

There is a good resemblance between the two curves, but with a slightly poorer value of S11 for the prototype. The values are -45 dB and -28 dB, respectively at the 2.1-2.6GHz band.

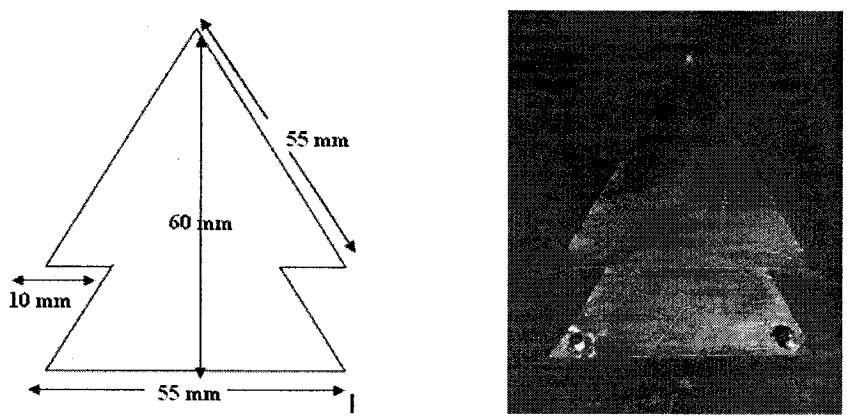

Figure 4.14 Proposed geometry of the triangular patch antenna.

4.6.1 RADIATION PATTERN AND AXIAL RATIO

The measured radiation pattern data are measured inside an anechoic chamber whereas the simulated radiation patterns are computed by the using Ansoft Ensemble simulation software [37]. Since the antenna losses are not small, the calculated directivity should not be nearly the same as the gain whereas the realized gain also includes impedance mismatch losses. The measured E-plane directivity is relatively higher as compared to the

simulated results. An approximate directivity can be calculated using equation (4.3). The measured directivity near the resonant frequency of 2.45 GHz is about 7.5 dB, with the simulation being in fair agreement at 8.5 dB. These small discrepancies probably caused by imperfect cutting of the patch and exact location of the probe feed. Also the height of solder pin of SMA connecter is a little bit higher than the height of substrate acting as a small dipole, resulting is higher values than expected. It can be explained that causes of these errors are the result of higher order modes; the patch is indeed operating in an undesired mode. Instead of operating in the dominant TM_{010} mode, the field from the patch radiates as if operating with a TM_{110} mode. This is determined by observing how the E-fields radiate on the surface of the patch. As illustrated in Figure 4-38, the field lines radiate off the corners of the substrate oppose to the flat edges for radiation with in a TM_{010} mode. This field line orientation is a classical exhibition of a patch operating in a TM_{110} mode, which is favorable for circular polarization. This explains the unusually large x-pol pattern that is uncommon for linear polarized antennas.

$$D = \frac{3200}{HP_E HP_H} \tag{4.3}$$

The radiation is circularly polarized. Fig 4.16 shows axial ratio at 2.2, 2.45 and 2.8 GHz verifying circular polarization, and is only measured in the principal planes corresponding to vertical (E-plane) and horizontal (H-plane) co- and cross-polarized components. Figs 4.17, 4.18, 4.19 and 4.20 shows radiation pattern at 2.45, 4.25 GHz, 5.4 and 5.8 GHz respectively. The E and H-plane patterns are symmetric, omni directional and stable as expected with the simulation results being in fair agreement.

The computed current distribution of the proposed antenna is shown in Fig. 4.20. Clearly currents are concentrated at the edges of the triangle. The combination of the two triangles creates unequal lengths for two separate current paths. These current paths correspond to two hybrid operating modes which result in wideband characteristics. The right-hand circularly polarized component is the dominant component here.

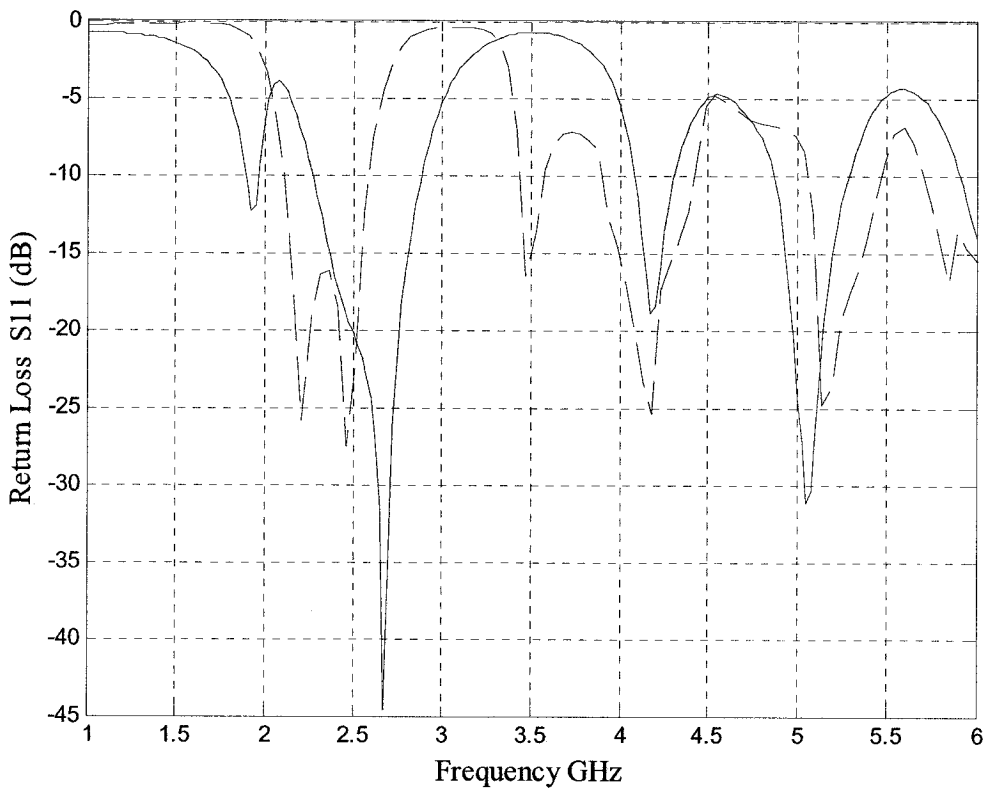

Figure 4.15 Return loss of the proposed triangular patch antenna.

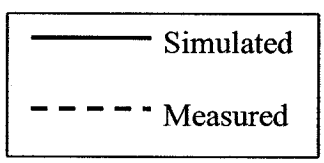

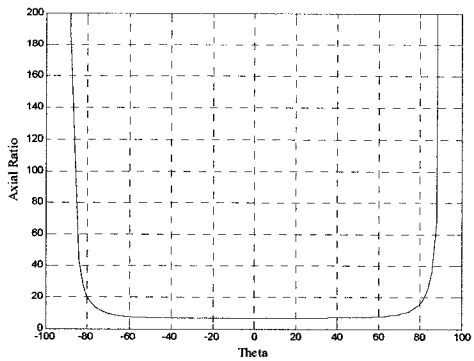

(a)

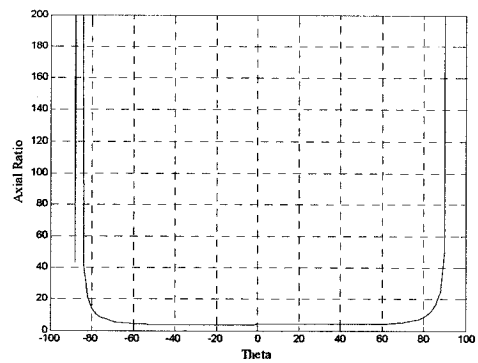

(b)

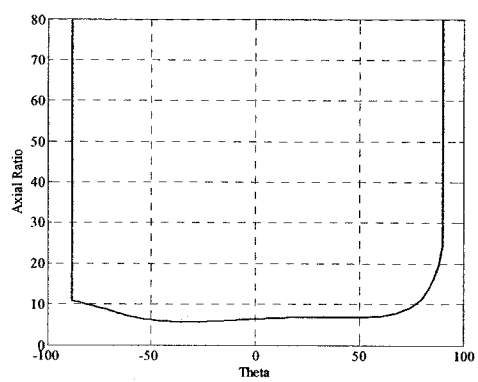

(c)

Figure 4.16 Axial ratio at (a) 2.2 GHz (b) 2.45GHz (c) 2.8GHz.

Simulated

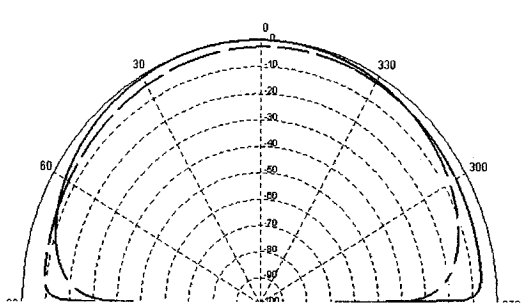

Measured

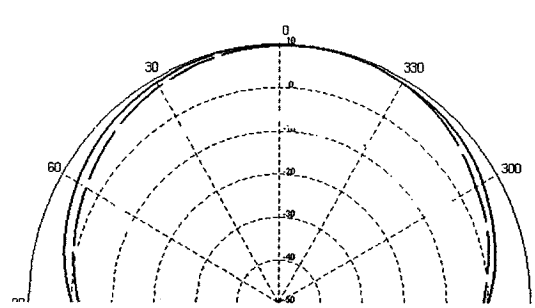

Figure 4.17 Comparison of the E-plane and H-plane antenna patterns at 2.45GHz.

Simulated Measured

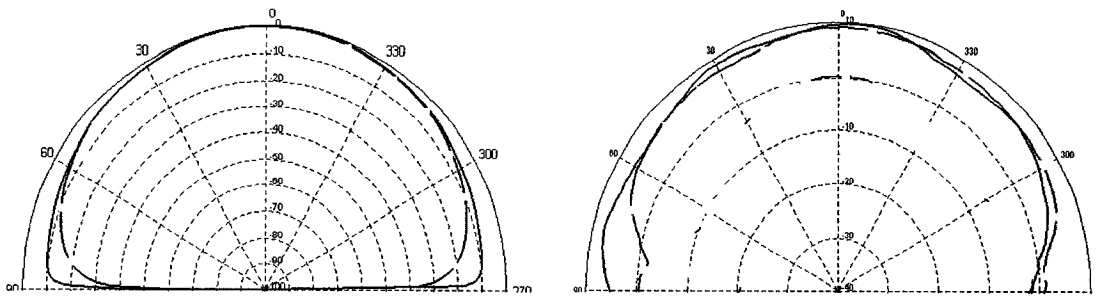

Figure 4.18 Comparison of the E-plane and H-plane antenna patterns at 4.25 GHz.

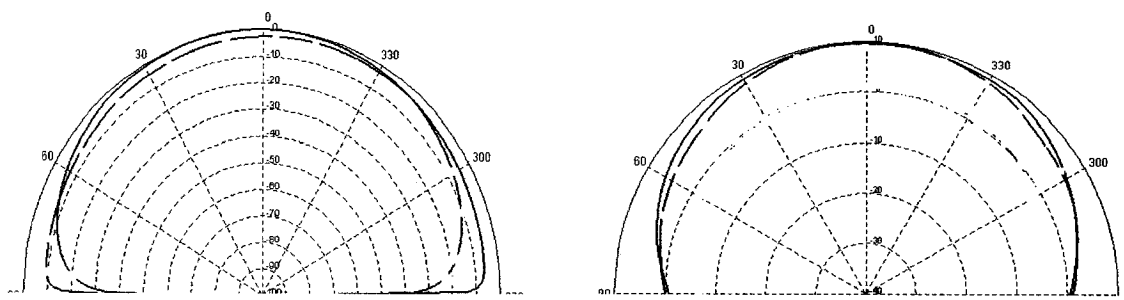

Figure 4.19 Comparison of the E-plane and H-plane antenna patterns at 5.4GHz.

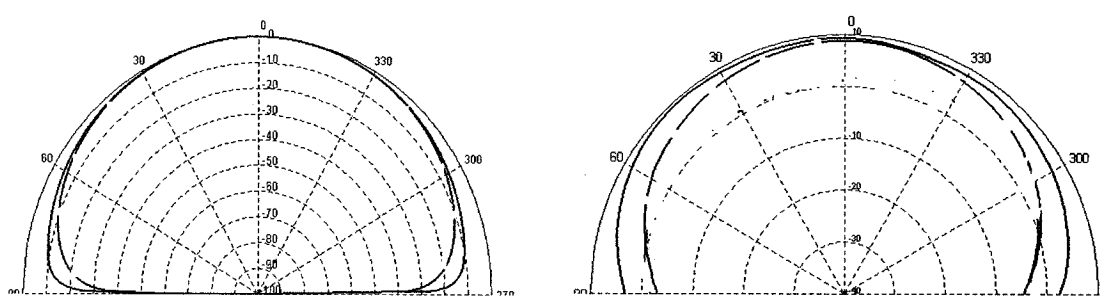

Figure 4.20 Comparison of the E-plane and H-plane antenna patterns at 5.8GHz.

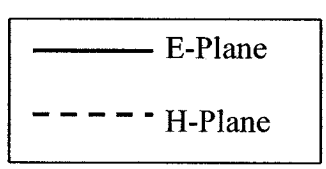

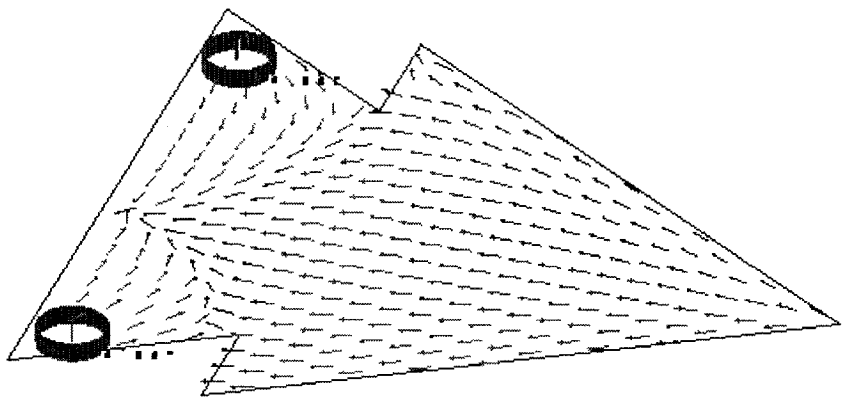

Figure 4-21 Current Distribution.

CHAPTER V - RECONFUGURABLE MICROSTRIP ANTENNA

5.1 INTRODUCTION

Reconfigurable antennas have recently received much attention for their applications in wireless communications, electronic surveillance and countermeasures, by adapting their properties to achieve selectivity in frequency, bandwidth, polarization and gain [21,28,33]. Compared to broad band antennas, reconfigurable antennas offer the advantages of compact size, similar radiation pattern for all designed frequency bands, efficient use of electromagnetic spectrum and frequency selectivity useful for reducing the adverse effects of co-site interference and jamming. Dual frequency reconfigurable microstrip antennas can offer additional advantages of frequency reuse for doubling the system capability and polarization diversity for good performance of reception and transmission or to integrate the receiving and transmitting functions into one antenna for reducing the antenna size [38]. Preliminary studies in reconfigurable microstrip antennas reported recently received great attention. A linearly polarized square spiral microstrip antenna capable of pattern and frequency reconfigurability was recently introduced [39]. A reconfigurable microstrip patch antenna using switchable slots for right hand and left hand circular polarization diversity was also studied [40]. An interesting approach of electronic tuning of a varactor integrated dual frequency coplanar strip dipole antenna is studied, which provides an attractive feature of electronic control [41]. However microstrip patch antennas having dual frequency operation and with broadband capabilities have not been much explored. Design of matching networks and the placement of switches are crucial in these types of antennas. A PIN diode controlled

switching technique for reconfigurable dual frequency operation has been recently reported [42]. This thesis presents novel compact design with different type of feeding techniques, reconfigurable, dual frequency, broadband, circularly polarized microstrip antenna that is capable of broad impedance bandwidth as well as reconfigurability for multiband operation by incorporating only one switch before the feed.

5.1.1 ANTENNA CONFIGURATION

A two-layer microstrip antenna with a novel feeding technique that uses all three most common type of feeding is designed. It uses only two substrates with same height, and dielectric constant of 2.2. Unlike the proposed antenna, published designs using two substrates with aperture coupling have much lower bandwidth [43–46] and do not easily allow for reconfigurability. The proposed configuration differs from conventional two-layer, microstrip-aperture coupled microstrip antennas in that the two substrates in the proposed configuration are not separated by a ground plane, and that a combination of feeding techniques is used resulting in enhanced bandwidth in addition to keeping feed dimensions small. In addition to the bandwidth advantage, the proposed configuration offers easy reconfigurability with the ability to exclude switches in the combination part of the feed. It also has an advantage in realizing active antennas. The feeding combination allows biasing of active devices without disturbing the main circuitry. The important aspect of this design is that it provides a high size reduction for all the operating frequencies, compared to conventional rectangular patches. No biasing circuitry is needed for this design, in which transmission lines can not be avoided in between the nonlinear components and radiating element, so that, added noise and ohmic losses are suppressed and the resulting structure is more compact. The radiation pattern,

gain and polarization are essentially unaffected by the frequency tuning, which is highly desirable for frequency reconfigurable microstrip antennas.

5.1.2 ANTENNA GEOMETRY

The geometry of the proposed reconfigurable antenna is show in Fig 5.1. The geometry of proposed antenna is very simple, consists of a semi circle with a slit in between, to help in producing broadband, multiband operations. Since the proposed antenna is reconfigurable, therefore it can be operated at 2.45 GHz, 3.25GHz, 3.5GHz, 4.75 GHz, 5.4GHz and 5.8GHz.

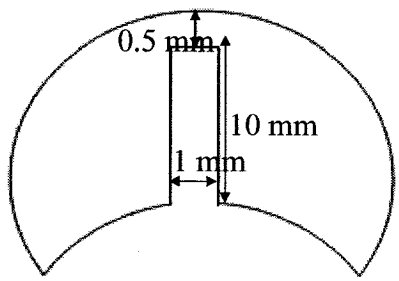

Figure 5.1 Geometry of the proposed antenna.

5.1.3 FEEDING TECHNIQUES

The proposed antenna is fed by all three common techniques as shown in Fig 5.2, where P1and P3 is probe feed, P2 is edge or microstrip line feed. P4-A and P4-B are electromagnetically coupled feed or proximity coupled using no contacting approach to the proposed antenna. Fig 5.3 shows 3D view of the proposed antenna and Fig 5.4 shows the top view of an antenna.

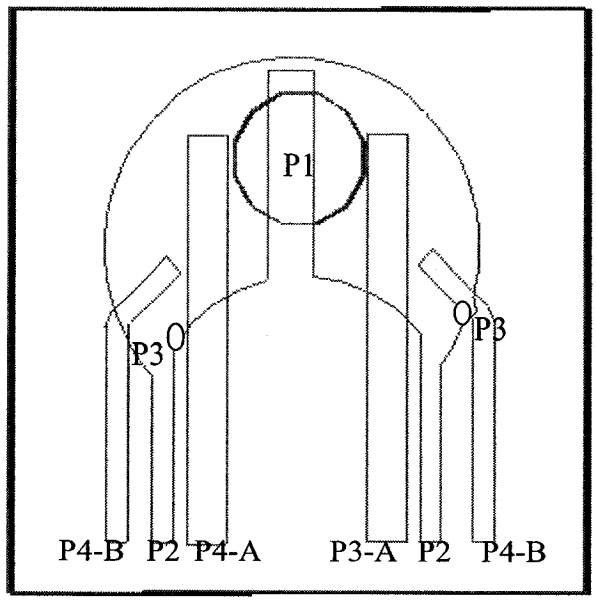

Figure 5.2 Top view of the reconfigurable antenna.

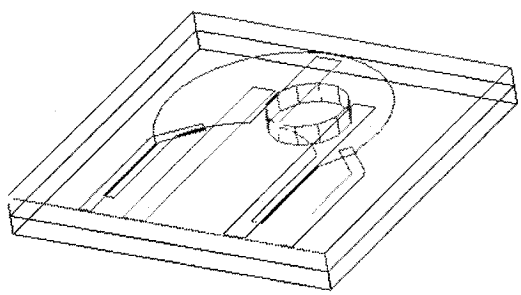

Figure 5.3 3-D view of the antenna.

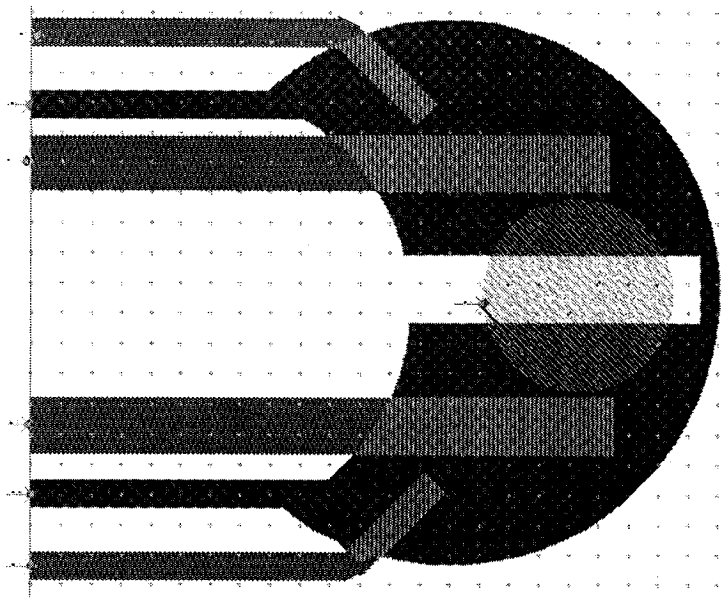

Figure 5.4 Top view of proposed antenna.

5.1.4 RADIATION PATTERN

If, an external microwave four-way switch is connected to all those four ports, then we can investigate radiation pattern and return loss, when the switch is on position 1, 2, 3, or 4 respectively. Due to complex feeding techniques and lack of resources only two out of four modes has been measured.

5.1.5 P1 IS ACTIVE

In this mode, antenna is fed by coaxial feed as shown in Fig 5.5. The return loss in this case is shown in Fig.5.6. The radiation pattern is in the broadside direction and is also omni directional. Fig 5.7 and 5.8 shows the respective gain of the proposed patch antenna at 5.4 and 5.8GHz. The gain of the antenna is about 7 dB for both operating frequencies. The return loss is better than -20 dB with broadband width of 4% and 0.86%, respectively.

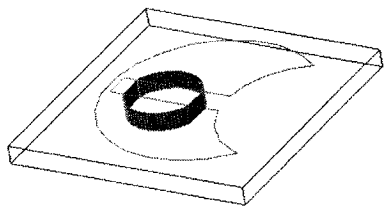

Figure 5.5 1) Mode 1 probe feed.

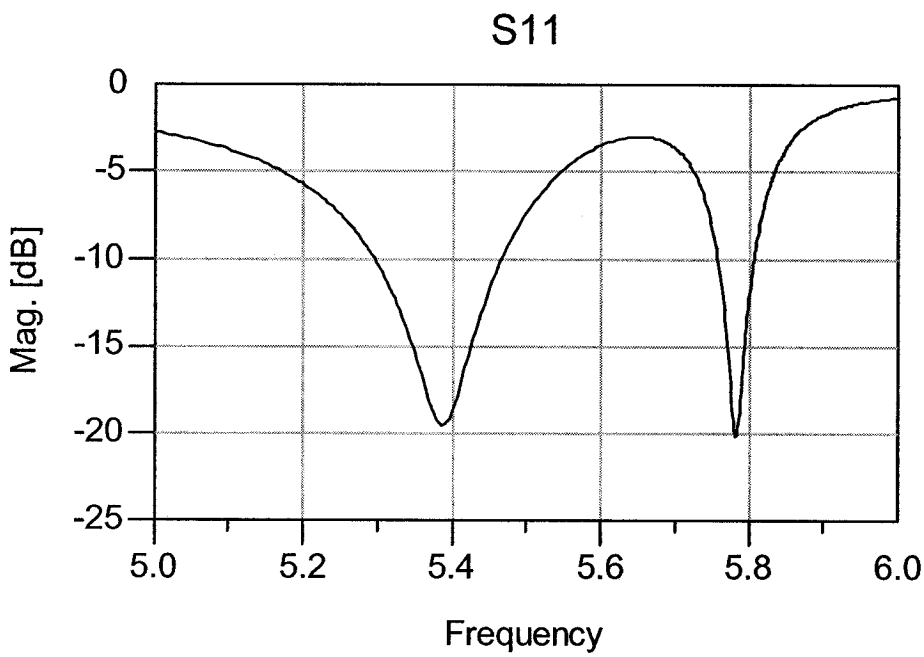

Figure 5.6 Return loss when SW1 is ON (probe feed).

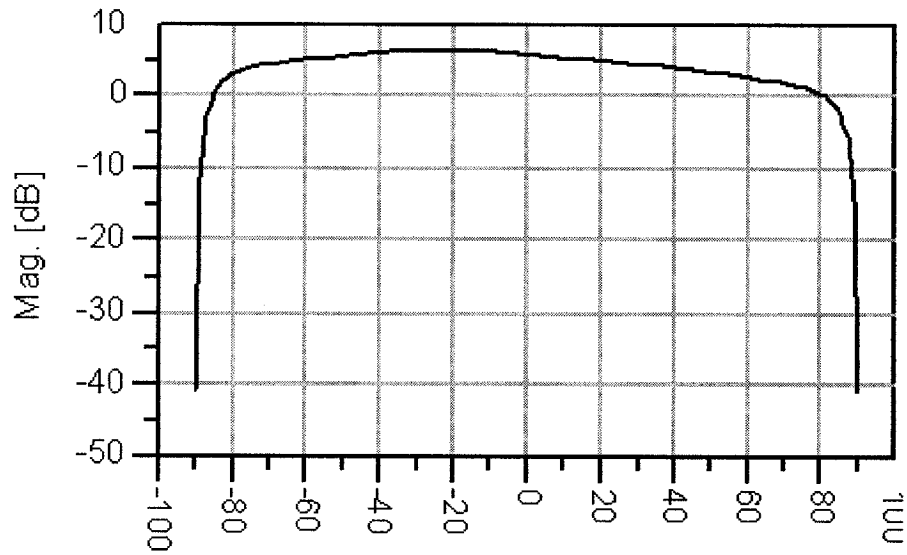

Figure 5.7 Gain at 5.4 GHz.

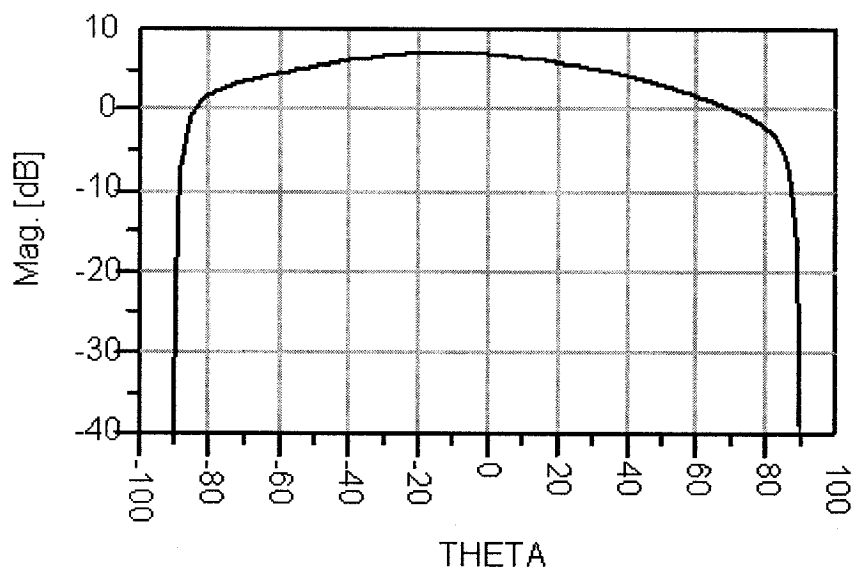

Figure 5.8 Gain at 5.8 GHz.

5.1.6 P2 IS ACTIVE

In this mode, antenna is fed by microstrip line feed as shown in Fig 5.9. The measurement and simulation result of input return loss is shown in Fig 5.10. The bandwidth from the measurement result is 17 % and the bandwidth using simulation result is 15%. The experimental result show the center frequency has been shifted up by 200 MHz. The resonance of the antenna can be seen by observing the dip in the return loss. There is some agreement between the simulation and measurement result for the bandwidth. The simulation results give a good approximation for the measurement even though the frequency has been shifted by 5% from the simulation result. The discrepancy between the simulation and measurement results can be attributed to the finiteness of the ground plane, which causes a shift in the resonance frequency and the fact that the response of the system is very sensitive to the exact location of the microstrip feed and the width of transmission line which is subject to alignment errors in the implementation process. Figures 5.11, 5.12, 5.13 show the radiation pattern of the antenna for H-Plane and E -Plane at 3.1 GHz. 3.4 GHz and 3.6 GHz respectively. The radiation pattern is in the broadside direction. The E-Plane pattern is almost the same as the H-Plane. The pattern is stable and omni directional. The measure and simulated co-pol patterns are almost similar at centre and side frequencies.. It is expected that this slight difference between simulated and measured data is due to inaccuracy in fabrication. These small discrepancies probably caused by imperfect cutting of the patch and exact width of transmission line feed. However, the strong similarities between the simulated and measured data indicate that the impedance match specification could be achieved using this antenna design.

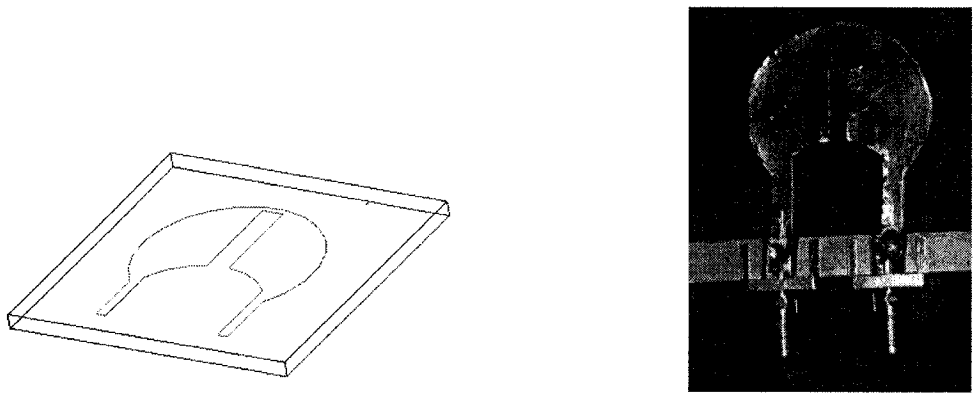

Figure 5.9 Mode 2, edge feed.

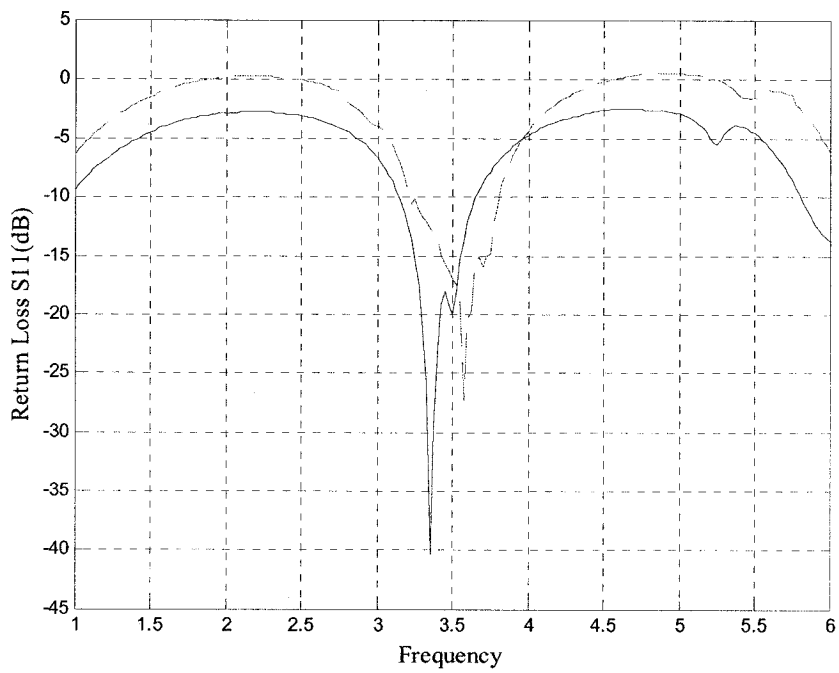

Figure 5.10 Return loss SW2 is on (microstrip line feed).

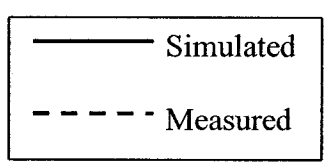

Simulated Measured

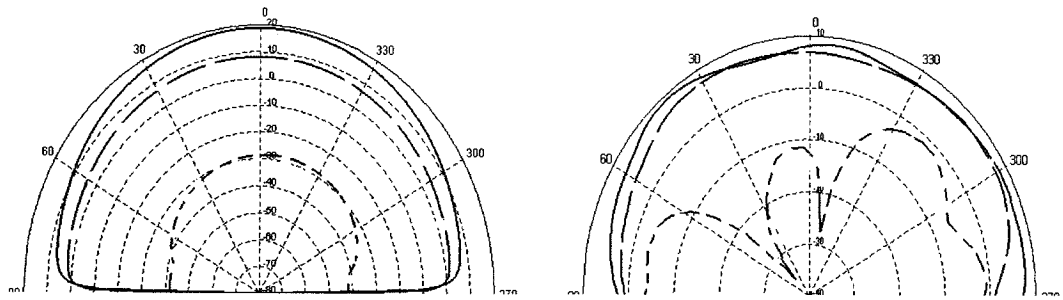

Figure 5.11 Comparison of the E-plane and H-plane co-pol and x-pol antenna patterns at 3.1 GHz.

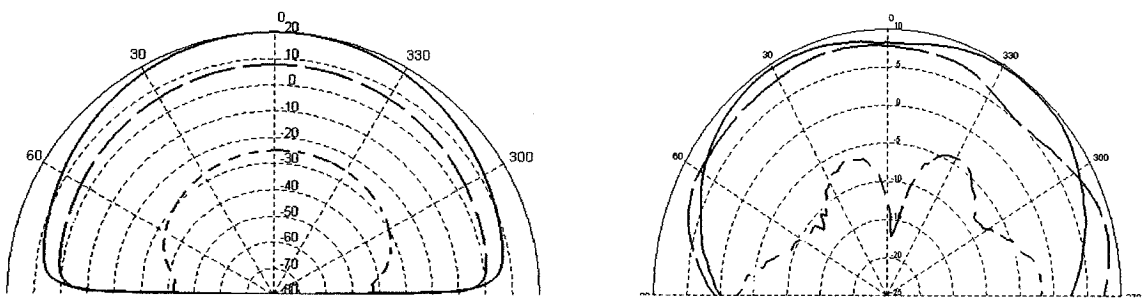

Figure 5.12 Comparison of the E-plane and H-plane co-pol and x-pol antenna patterns at 3.4 GHz.

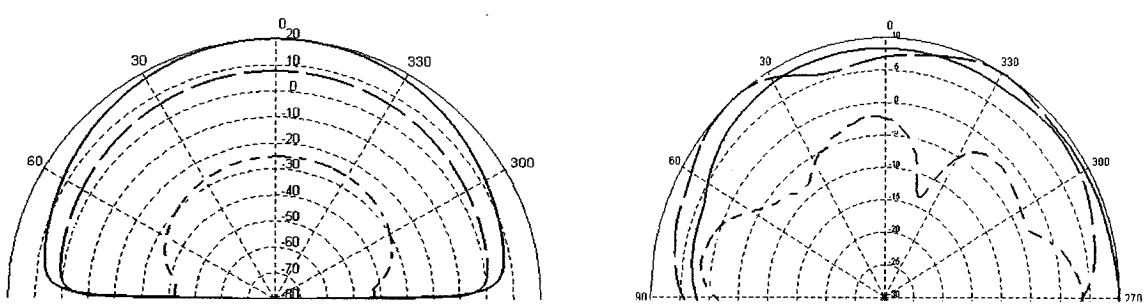

Figure 5.13 Comparison of the E-plane and H-plane co-pol and x-pol antenna patterns at 3.6 GHz.

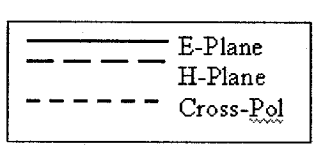

5.1.7 P3 IS ACTIVE

In this mode, antenna is fed by two coaxial feed as shown in Fig 5.14. The measurement and simulation result of input return loss is shown in Fig 5.15. On this mode the antenna is operating at two frequencies. The experimental result show the frequency has been shifted up by 10 MHz. There is an agreement between the simulation and measurement result for the return loss. The simulation results give a good approximation for the measurement even though the frequency has been shifted slightly from the simulation result. The slight discrepancy between the simulation and measurement results can be attributed to the finiteness of the ground plane, which causes a shift in the resonance frequency and the fact that the response of the system is very sensitive to the exact location of the probe feed which is subject to alignment errors in the implementation process. Figures 5.16, and 5.17 show the radiation pattern of the antenna for H-Plane and E-Plane at 3.1 GH. 3.1GHz and 3.6 GHz respectively. The radiation pattern is in the broadside direction. The E Plane pattern is almost the same as the H Plane. The pattern is stable and omni directional. The measure and simulated co-pol patterns are almost similar at centre and side frequencies. It is expected that this slight difference between simulated and measured data is due to inaccuracy in fabrication. These small discrepancies probably caused by imperfect cutting of the patch and exact location of the probe feed. However, the similarities between the simulated and measured data indicate that the impedance match specification could be achieved using this antenna design.

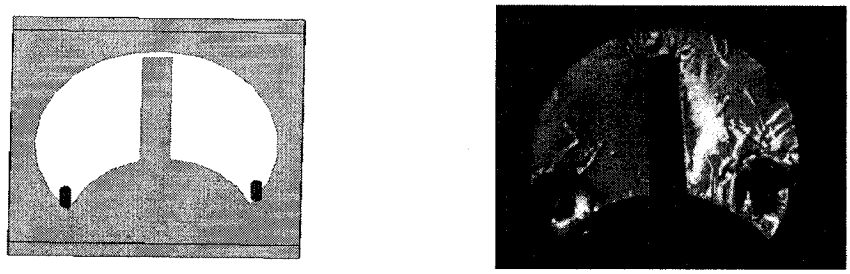

Figure 5.14 Mode 3, probe feed.

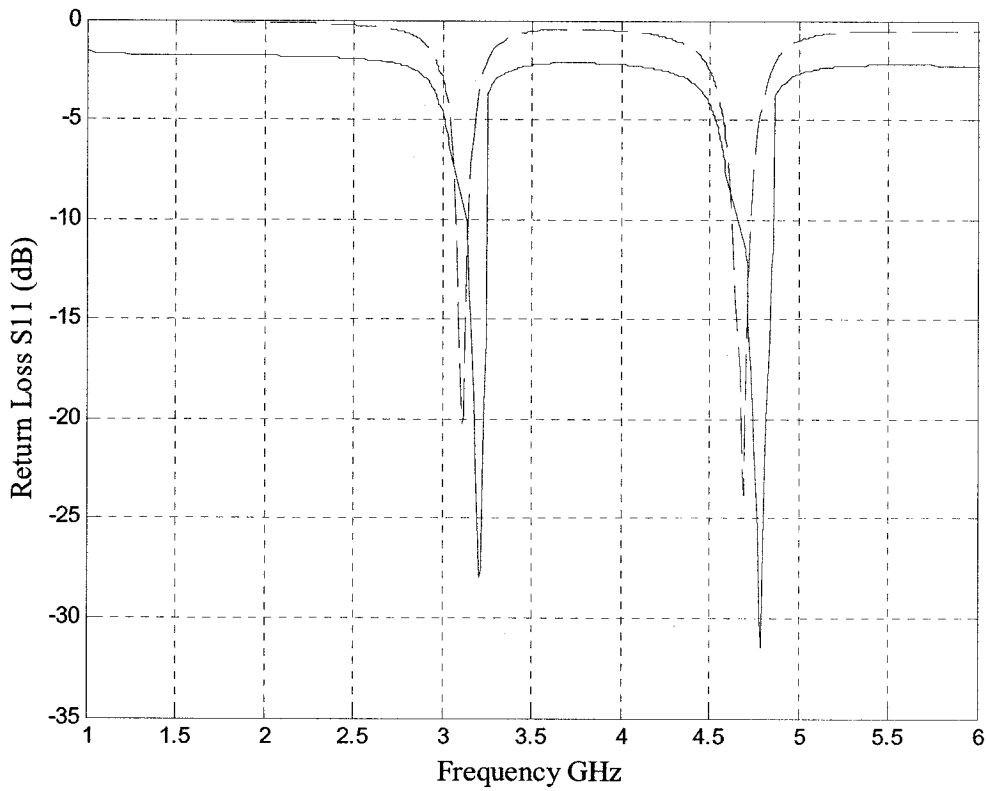

Figure 5.15 Return loss.

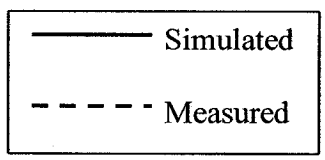

Simulated Measured

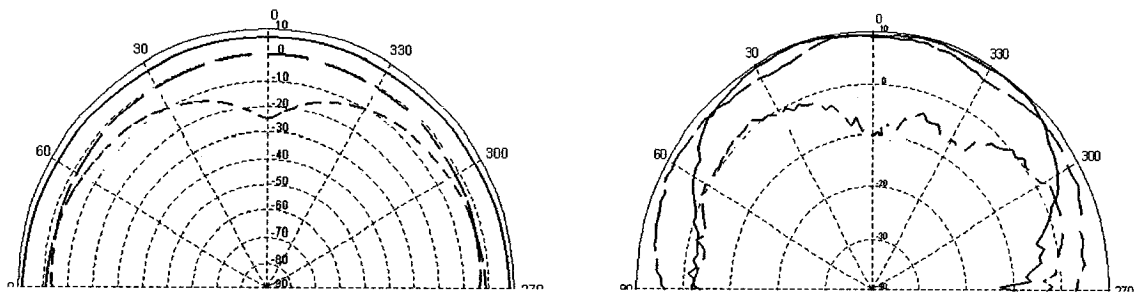

Figure 5.16 Comparison of the E-plane and H-plane co-pol and x-pol antenna patterns at 2.8GHz.

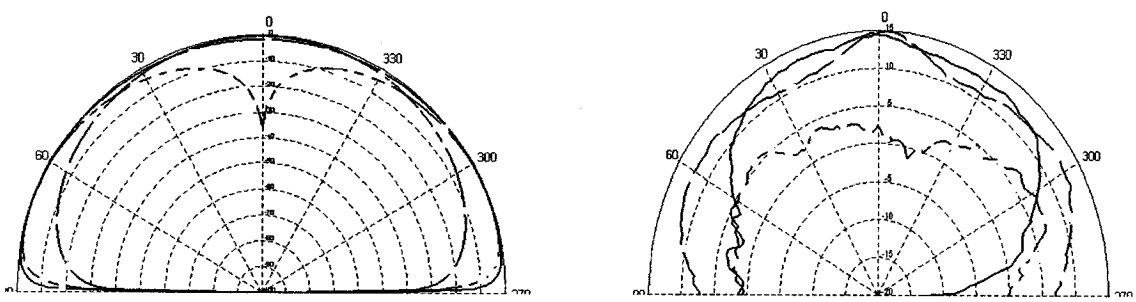

Figure 5.17 Comparison of the E-plane and H-plane co-pol and x-pol antenna patterns at 2.8GHz.

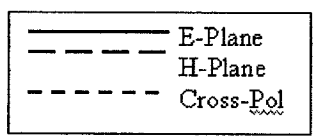

5.1.8 P4-A IS ACTIVE

In this mode antenna is fed by proximity couple feed as shown in Fig 5.18. The return loss in this case is shown in Fig 5.19. Fig 5.21 shows the gain of the antenna. The gain of the antenna is about 6 dB. The radiation pattern is in the broadside direction, and is omni directional. The return loss is better than -30 dB. Finally Fig 5.20 shows the axial ratio at center frequencies which is 0 dB verifying linear polarization

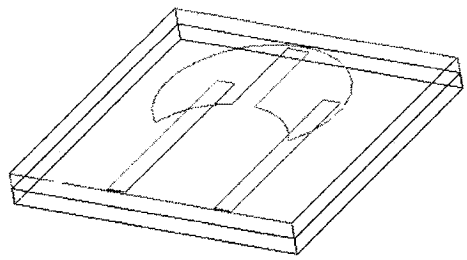

Figure 5.18 Mode 4-A, coupled feed.

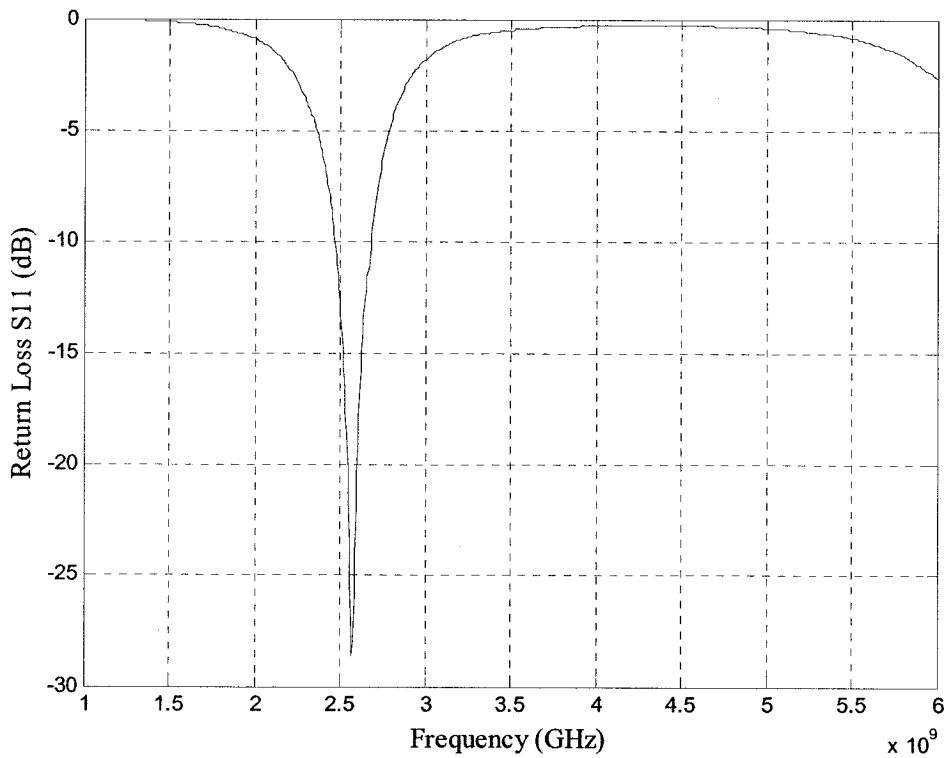

Figure 5.19 Return loss SW2 is on (proximity coupled feed).

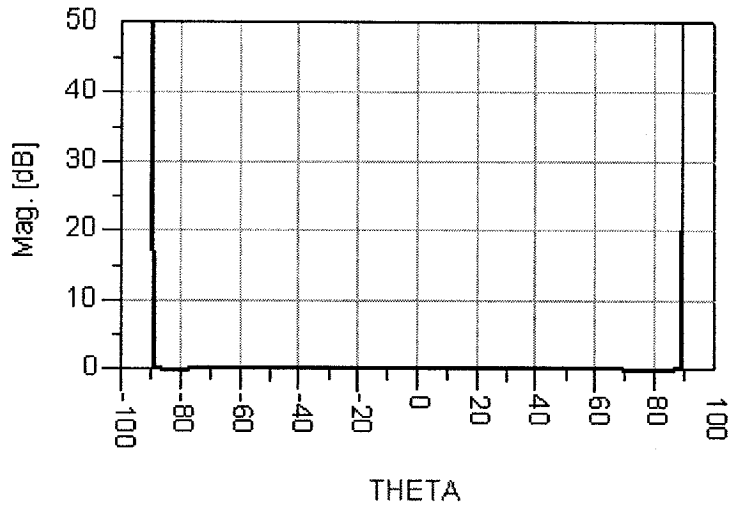

Figure 5.20 Axial ratio.

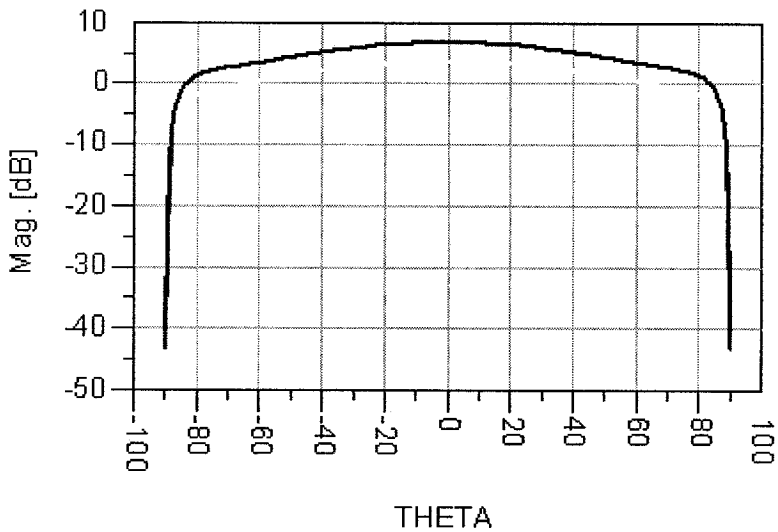

Figure 5.21 Gain of the antenna.

5.1.9 P4-B IS ACTIVE

In this mode, antenna is fed by angular coupled feed as shown in Fig 5.22. The return loss in this case is shown in Fig 5.23. Fig 5.25 shows the gain of the antenna. The gain of the antenna is about 8 dB. The radiation pattern is in the broadside direction, and is omni

directional. The return loss is better than -30 dB. Finally Fig 5.24 shows the axial ratio at center frequencies which is approx equal to 1 dB verifying circular

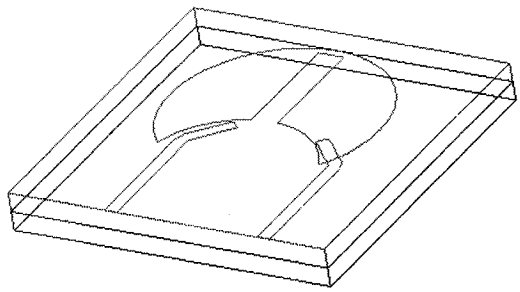

Figure 5.22 Mode 4-B, angular coupled feed.

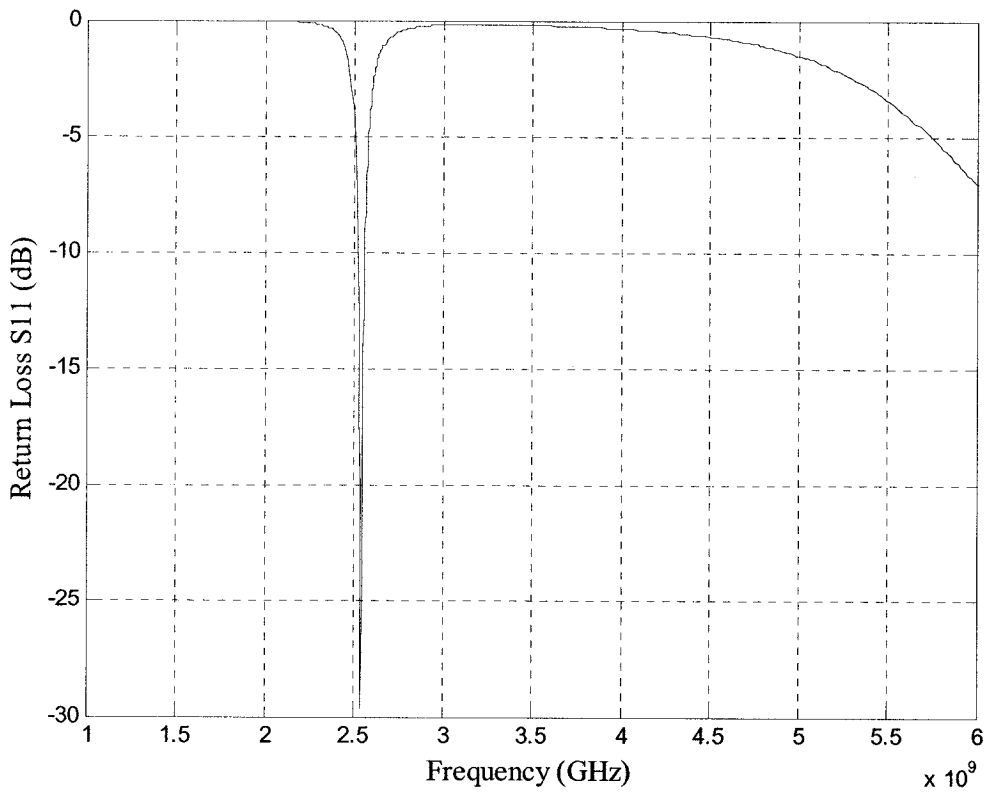

Figure 5.23 Return loss SW2 is on (proximity coupled feed with 90° bend).

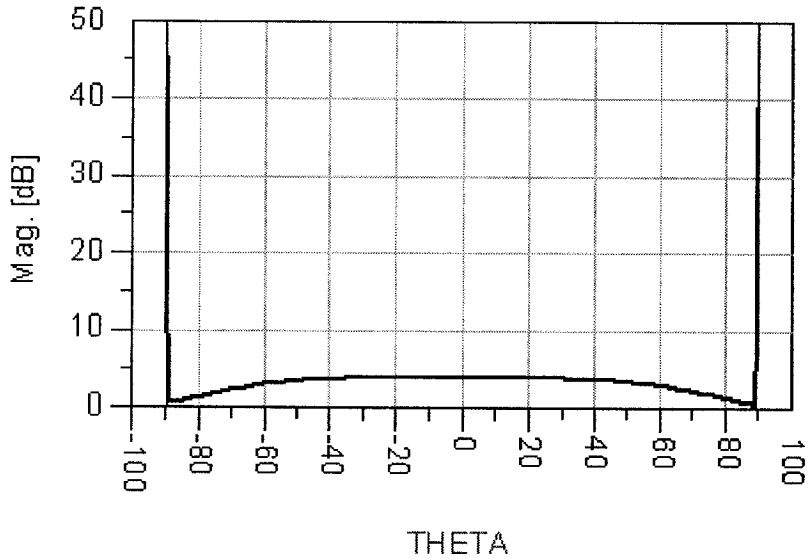

Figure 5.24 Axial ratio.

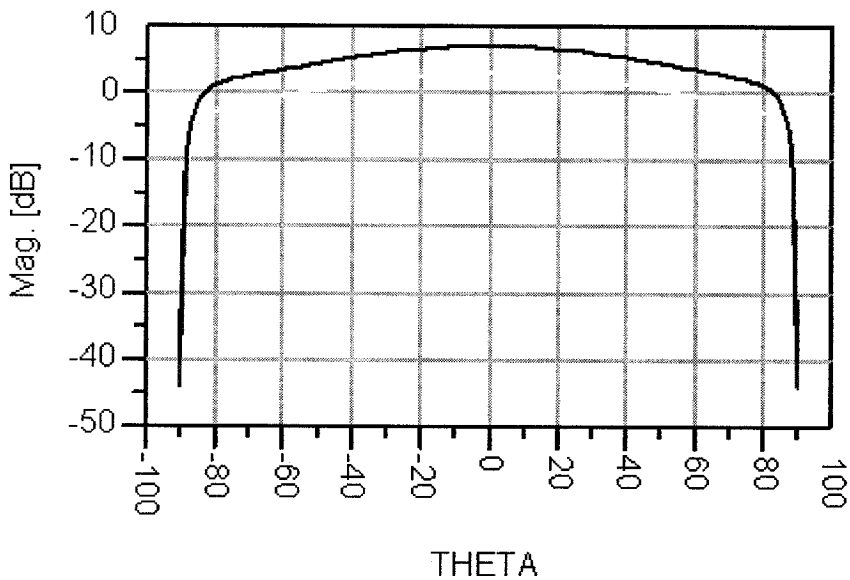

Figure 5.25 Gain of the antenna.

CHAPTER VI - CONCLUSION AND FUTURE WORK

6.1 CONCLUSION

In this thesis, three broadband antennas are successfully implemented using the multiple resonance technique. The shapes of patch antennas used are rectangular, circular and triangular. The resonant technique using multiple patches not only produces circular polarization patterns but also gives the bandwidth up to 28.5%, 21.73% and 19.86% respectively, with gain better than 7 dB. All the proposed antennas meet all the goals of this thesis which are to design a reduced size, multi-broadband, circularly polarized, easy to fabricate, WLAN, microstrip antennas.

The use of multiple patch microstrip antennas gives better performance than single patch antennas. This is due to the multiple-resonant lengths that are perpendicular to each other to produce dual polarizations. The developed microstrip antennas have performed adequately and managed to meet the specifications. The designed antennas showed potential as a candidate for use in WLAN environments where high directivity and low grating lobes are expected. Reduction in size and easy to fabricate designs may lead to such a standard. The performance of the antenna can be further improved by using substrates with low insertion losses as well the emergence of improved design techniques.

Also, a reconfigurable antenna is designed that possesses frequency and polarization reconfigurability. The geometry of the antenna is very simple with different feeding technique and the reconfigurability is achieved using an external switch. Depending upon the switch location and implementation, the antenna operates in a number of useful

modes. The same basic antenna with same switch can be operated at single or dual band frequencies. This functionality is of particular interest in a network environment where an antenna is required to transmit and receive in different frequency bands. The antenna may also be used in applications requiring frequency diversity effectively, yet inexpensively.

6.2 FUTURE WORK

In order to achieve good directivity levels, the current design should be improved. Moreover, the antenna system can be extended to higher frequencies to accommodate for future high speed WLANs. To facilitate higher transmission rates, with good directivity an array antenna would be the best choice also beam steering capabilities can be developed to support high speed switching and to avoid multipath dispersion inherent in WLAN where there are many reflective surface. It is expected however that further work is required in order to improve the current broadband antennas.

The use of parasitic rings can be use in order to broadband narrowband antennas because of its ease of implementation. Other schemes utilizing patches with slotted gaps and circles with slotted lines have been known to perform effectively under broadband situations. Also, the external microwave switch is currently being suggested but RF MEMS switch may be implemented.

REFERENCES

[1] M. George J and Deepuku, et al, Broadband dual frequency antenna , Electronic Letter, Vol. 1, page: 1531 – 1532, 1996.

[2] S. Maci and G. Biffi Gentili, Dual frequency patch antenna , IEEE Antenna and Propagation Magazine, Vol. 39, No. 6, page: 13 – 19, 1997.

[3] J. Y. Jan and K. L. Wong, Single feed dual frequency circular microstrip antenna with an open ring slot , Microwave Optic Technology Letter, 22, page: 157 – 160, 1999.

[4] K. B. Heish and M. H. Chen, Single feed dual band circularly polarized microstrip antenna ,Electronic Letters 34, page: 1170 – 1171, 1998.

[5] M.F. Iskander, J.C. Langer, J. Mathews, Wideband dipole antenna for WLAN , IEEE antennas and Propagation Society Symposium 2004, Volume 2, page(s):1963 – 1966, 20-25June 2004.

[6] Q. Zhong, Y. Li, H. Jiang, Y. Long, Design of a novel dualfrequency microstrip patch antenna for WLAN applications , IEEE Antennas and Propagation Society Symposium 2004, Volume 1, page(s):277 – 280, 20-25 June 2004.

[7] K.L Wong Compact and Broadband Microstrip Antennas, A Wiley-Inter Science Publication John Wiley & Sons- Inc 2002

[8] D. L. Sengupta, Resonant Frequency of a Tunable Rectangular Patch Antenna, Electronics Letters, Vol. 20 pp. 614-615, 1984.

[9] N. Fayyaz, S. Safavi-Naeini, E. Shin, N. Hodjat, A Novel Electronically Tunable Rectangular Patch Antenna with One Octave Bandwidth, Proceedings of IEEE

Canadian Conference on Electrical and Computer Engineering, Vol. 1, pp. 25-28, 1998.

[10] S. H. Al-Charchafchi, M. Frances, Electronically Tunable Microstrip Patch Antennas, IEEE Antennas and Propagation Symposium Digest ,Vol. 1, pp. 304-307, 1998.

[11] K. A. Jose, V. K. Varadan V. V. Varadan, Experimental Investigations on Electronically Tunable Microstrip Antennas, Microwave and Optical Technology Letters, Vol. 20, pp. 166- 169, 1999.

[12] L. Stutzman and G.A Thiele, Antenna Theory and Design, 2nd ed: John Wiley & Sons, Inc., 1998.

[13] C.A Balanis, Antenna Theory Analysis and Design, 2nd ed: John Wiley & Sons, Inc., 2001.

[14] E.R Brown and C.D Parker, Radiation Properties of a Planar Antenna on a Photonic-Crystal Substrate, J Opt Soc Am B, vol. 10, 1993

[15] D. M. Pozar, and B. Kaufmann, Increasing the Bnadwidth of a Microstrip Antenna by Proximity Coupling, Electron. Lett, vol.23, No. 8, pp. 368- 369., 1987.

[16] N. G. Alexopoulos and D. R. Jackson Fundamental superstrate (cover) effects on printed circuit antennas, IEEE Trans. Antennas and Propagation, Vol. AP-32, pp 807-816, August 1984.

[17] B. Robert, T. Razban, and A. Papiernik, Compact amplifier integration in square patch antenna, Electronics letters, Vol. 28, pp. 1808-1810, Sept. 1992.

[18] R. Q. Lee and K. F. Lee Experimental study of the two-layer electromagnetically coupled Rectangular patch antenna IEEE Trans. Antennas and Propagation, Vol. 38,

pp. 1298-1302, Aug. 1990.

[19] T. Huynh and K. F. Lee, Single layer single patch wideband microstrip patch antenna, Electronics Letters, Vol. 31, pp. 1310-1311, August 1995.

[20] V. Gupta, S. Sinha, S. K. Koul and B. Bhat, Wideband dielectric resonator-loaded suspended microstrip patch antennas, Microwave and Optical Technology Letters, Vol. 37, pp. 300-302, May 2003.

[21] K.L Wong, Compact and Broadband Microstrip Antennas, John Wiley & Sons, New York, 2002.

[22] Y. M. Jo, Broadband patch antennas using a wedged-shaped air dielectric substrate, in IEEE Antennas Propagation Soc. Int. Symp. Dig., pp. 932-935, 1999.

[23] P. K. Singhal and L. Shrivastava, On the investigations of a wide band proximity fed bow tie shaped microstrip antenna, Journal of Microwave and Optoelectronics , Vol. 3, pp. 87-98, April 2004.

[24] K. M. Luk, L. K. Au Yeung, C. L. Mak and K. F. Lee, Circular patch with an L shaped probe, Microwave and Optical Technology Letters, Vol. 20, pp. 356-257, February 1999.

[25] K. L. Wong and W. H. Hsu, Broadband triangular microstrip antenna with U-shaped slot Electronics Letters, Vol. 33, pp. 2085-2087, December 1997.

[26] G. Kumar and K.C. Gupta, Directly coupled multiple resonator wide-band microstrip antennas, IEEE Trans. Antennas and Propagation, Vol. 33, pp. 588-593, June 1985.

[27] R. B. Waterhouse, Design of probe-fed stacked patches, IEEE Trans. Antennas Propagat. Vol. 47, pp. 1780-1784, Dec. 1999.

[28] R.Garg [et al], Microstrip antennas design handbook, Boston, MA : Artech House, 2001.

[29] D.M. Pozar, Microwave Engineering, John Wiley & Sons, New York, 1998

[30] M. Haneishi and S. Yoshida, A Design Method of Circularly Polarized Rectangular Microstrip Antenna by One-Point Feed, in Microstrip Antenna Design, K. C. Gupta and A. Benalla (Eds.), Artech House, Norwood, MA,Vol. 3, pp. 313-321, 1988.

[31] R. E. Munson, Conformal Microstrip Antennas and Microstrip Phased Arrays, IEEE Trans. On Antennas and Propagation, vol. 22, No. 1, pp.74-78. , 1974.

[32] T. Huynh and K.F. Lee, Single-layer single patch wideband microstrip antenna Electronics Lett., Vol.31, pp. 1310-1312, Aug. 1995.

[33] G. Kumar and K.C. Gupta, Directly coupled multiple resonator wideband microstrip antennas, IEEE Trans. Antennas Propagat., Vol. 33, pp. 588- 593, June 1985.

[34] F. Yang, X.X. Zhang, X. Ye and Y. Rahmat-Samii, Wide-band E-shaped Patch Antennas for wireless communications IEEE Trans. Antennas Propagat., Vol.49, pp. 1094-1100, July 2001.

[35] S.A. Long and D.M. Walton, A dual-frequency stacked circular-disc antenna, IEEE Trans. Antennas Propagat., Vol. 27, pp. 270- 273, Mar. 1979.

[36] D.M. Pozar, A microstrip antenna aperture coupled to a microstrip lines, Electronics Lett., Vol. 21,pp. 49-50 Jan. 1985.

[37] Ansoft Corporate, 225 West Station, Square Drive, Suite 200, Pittsburg PA, http://www.ansoft.com Last Visited 17 Feb. 2007

[38] D. Peroulis, K. Sarabandi, and P. B. K. Katehi, Design of recon.gurable slot antennas, IEEE Transactions on Antennasand Propagation, Vol. 53, 645–654,

2005.

[39] F. S. Zhang, and J. T. Bernhard, A novel radiation pattern and frequency recon.gurable single turn square spiral microstrip antenna, IEEE Microwave and Wireless ComponentsLetters, Vol. 13, 57–59, 1998.

[40] F. Yang, and Y. Rahmat-Samii, A recon.gurable patch antenna using switchable slots for circular polarization diversity, IEEE Microwave and Wireless Components Letters, Vol. 12, 96–98, 2002.

[41] A. T Kolsrud, M. Y. Li, and K. Chang, Dual-frequency electronically tunable CPW-fed CPS dipole antenna, Electronics Letters, Vol. 34, 609–611, 1998.

[42] S.V Shynu, G. Augustin, C. K. Aanandan, P. Mohanan, and K. Vasudevan, A compact electronically reconfigurable dual frequency microstrip antenna for L-band applications, International Journal on Wireless and Optical Communications, Vol. 2, No. 2, 181–187, 2004.

[43] W. Menzel, and W. Grabherr, A microstrip patch antenna with coplanar line feed, IEEE Microwave and Guided Wave Letters, Vol. 1, 340–342, 1991.

[44] R. Smith, and J. T. Williams, Coplanar waveguide feed for microstrip patch antennas, Electronics Letters, Vol. 28, 2272– 2274, 1992.

[45] S.M Deng, M. D. Wu, and P. Hsu, Analysis of coplanar waveguide-fed microstrip antennas, IEEE Trans. Antennas and Propagation, Vol. 43, 734–737, July 1995.

[46] L.Giau.ret,, J. Laheurte, and A. Papiernik, Study of various Progress In Electromagnetics Research, PIER 55, 2005 239 shapes of the coupling slot in CPW-fed microstrip antennas, IEEE Trans. Antennas and Propagation, Vol. 45, 642–647, April 1997.

[47] K. Hirasawa, M. Haneishi, Analysis, Design, and Measurement of Small and Low-Profile Antennas. Chapter 4: Suzuki, Y. Key Points in the Design and Measurement of Microstrip Antennas. Artech House, Boston, 1992.

[48] S.A Schelkunoff, Electromagnetic Waves, Van Nostrand, New York, Chap 10,1943.

[49] M. Cuhaci, and D.S James, Radiation From Triangular and Circular Resonators in Microstrip, IEEE MTT-S Int. Microwave Symp. Vol. 77, pp.438-441, 1997.

[50] J.Helszajn, and D.S.James,Planer Triangular Resonators With Magnetic Walls,IEEE Trans. OnMicrowave Theory and Techniques, Vol. MTT-26, pp.95-155, 1978.

[51] J. Helszajn, and D.S.James and W.T Nisber, Circulators Using Planer Triangular Resonators, IEEE Trans On Microwave Theory and Techniques, Vol. MTT-27, pp 188-193, 1979.

[52] I.J Bahl and P.Bhartia, Microstrip Antenna, Artech House, Dedham, M.A.1980

[53] W.K Chen, F.Lee and J.S Dahele, Theoretical and Experimental Studies of the Resonant Frequencies of the Equilateral Triangular Microstrip Antenna, IEEE Trans. On Antennas and Propagation, Vol. Ap-40pp 1253-1256, , 1992

APPENDIX A - ANAYLYSIS OF MICROSTRIP ANTENNAS

A.1 ANALYSIS OF CIRCULAR PATCH ANTENNA

One method commonly used to model microstrip antennas is the Magnetic Cavity Model [47]. The cavity model of the MSA assumes that the patch and the ground plane are electric walls, and the periphery of the patch is a magnetic wall. The fields in the resulting cavity are assumed to be the fields of the antenna and Huygen's Principle is applied at the magnetic wall to determine radiation. To determine the fields within the cavity, a solution of an inhomogeneous wave equation is required. Therefore, the Magnetic Cavity Model is most easily applied when the method of separation of variables is applicable. The circular patch MSAs are symmetric in two planes. Therefore, the cavity model is convenient. For arbitrarily shaped patches, application of the Method of Moments to the integral equation is necessary to avoid tedious calculations. The magnetic cavity model works best for a thin substrate. In this case the TM modes are superior in the cavity. The cavity model makes the following assumptions:

The electric field is z-directed, and the magnetic field has only a transverse component in the cavity. Since the substrate is assumed thin, the fields in the cavity do not vary with z. The tangential component of the magnetic field is negligible at the edge of the patch. The existence of a fringing field can be accounted for by slightly extending the edges of the patch. An arbitrarily shaped microstrip patch is illustrated in Figure A.1. The substrate thickness, t, is thin. The circumference of the patch is C and the area bounded by the circumference is S. The unit vector, n, is normal to the patch edge. The substrate has a dielectric constant ε_r.

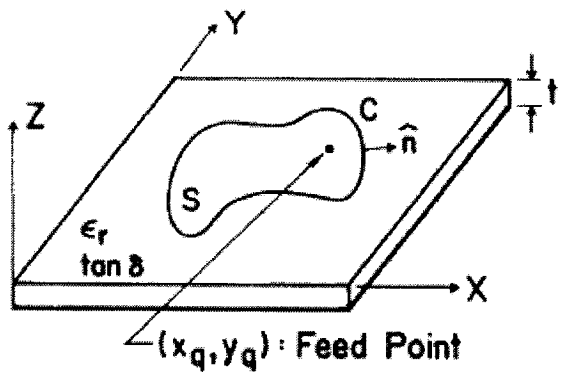

Figure A.1 arbitrarily shaped microstrip patch antenna.

If an e^{jwt} time variation is assumed, the fields from a z-directed current source at the point (x_q,y_q) satisfy the following relations:

$$(\nabla_T^{\ 2} + k^2)E_z = -j\omega\mu_o j_z(x_q, y_q) \tag{A.1}$$

$$H = \frac{j}{\omega\mu_o} \nabla_T X(a_z E_z) \tag{A.2}$$

where $k = k_o\sqrt{\varepsilon_r}$ (A.3)

where k_o is the wave number.

Both (A.1) and (A.2) are derived using Maxwell's Equations. The electric wall condition is automatically satisfied at the patch and ground plane because the electric field is defined as perpendicular to both. The magnetic wall condition is satisfied at the edges of the patch if

$$\frac{\partial E_z}{\partial n} = 0 \tag{A.4}$$

The expression in (A.2) is an inhomogeneous wave equation that can be solved by finding eigen functions, satisfy the following homogeneous wave equation

$$(\nabla^2{}_T + (k^{(1)})^2)\varphi^{(1)} = 0 \qquad \text{(A.5)}$$

The magnetic cavity model is also readily applied to a circular patch antenna of radius a, and feed point location A, as illustrated in Fig A.2 . In this case the solution to (A.5) is given by

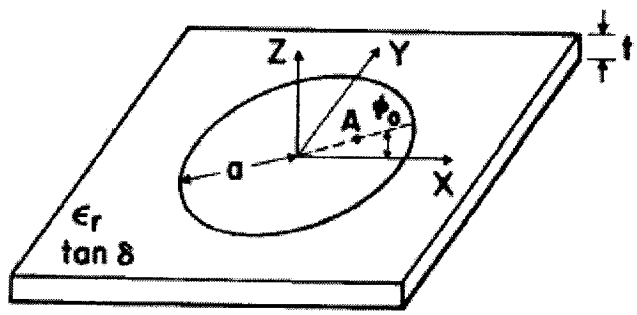

Figure A.2 Configuration of a circular disk microstrip antenna.

$$\varphi_{mn}(r,\phi) = \frac{\delta_m k_{mn}}{\chi_{mn}\sqrt{\pi(1-\frac{m^2}{\chi_{mn}^2})J_m(\chi_{mn})}} J_m(k_{mn}r)\cos(m(\phi-\phi_o)) \qquad \text{(A.6)}$$

where k_{mn} is the eigenvalue corresponding to mode TM_{mn}, and is the nth root of J_m (mn) The prime refers to the derivative on the argument. The function $J_m(x)$ is the Bessel function of order m. Some values of are found in Table A.1.

	n=0	n=1	n=2	n=3
m=1	3.832	1.841	3.054	4.201
m=2	7.016	5.331	6.706	8.015

Table A.1. Some lower roots of $J_m(\chi_{mn})$.

The values of χ_{mn} are used to find the eigen values, k_{mn}, using

$$k_{mn} = \frac{\chi_{mn}}{a_{mn}} \tag{A.7}$$

where a_{mn} is the effective patch radius, lengthened to account for fringing fields at the edge of the patch. Once again, the cavity electric field is found by substituting solutions to (A.6) into (A.8) and (A.9).

$$E_z(x,y) = \sum_{l=1}^{N} A^{(l)} \varphi^{(l)}(x,y) \tag{A.8}$$

For an antenna with one input terminal, the values of the coefficients are expressed as

$$A^{(l)} = \frac{\sqrt{2S_e}}{t} \frac{M^{(l)*}}{j\omega C + \frac{1}{j\omega L^{(l)}} + g^{(l)}} I_q \tag{A.9}$$

Where

$$M^{(l)} = \sqrt{S_e}\varphi^{(l)}(x,y)$$

$$C = \varepsilon_r \varepsilon_o \frac{S_e}{t}$$

$$L^{(l)} = \frac{1}{(\omega^{(l)})^2 C}$$

and

$$\omega^{(l)} = \frac{k^{(l)}}{\sqrt{\varepsilon_r \varepsilon_o}}$$

The expression for the electric field in the cavity is

$$E_z(r,\phi) = \sum_m \sum_n \frac{V_{mn}}{t} \frac{J_m(k_{mn}r)}{J_m(\chi_{mn})} \cos(m(\phi - \phi_o) \tag{A.10}$$

Where

$$V_{mn} = \frac{\sqrt{2}\delta_m^2 I_q}{j\omega C + \frac{1}{j\omega L_{mn}} + g_{mn}} \left(\frac{J_m(k_{mn}r)}{J_m(\chi_{mn})} \right) \left(\frac{1}{1 - \left(\frac{m^2}{\chi_{mn}^2} \right)} \right) \tag{A.11}$$

and the variables are identical to those used for the rectangular patch except that the feed point is denoted using the cylindrical coordinates. The input impedance of the circular patch antenna is found using (A.12) and is given by

$$H_o^{(1)} = \frac{-j\omega\varepsilon_o}{4\pi} t \left(2\cos\left(\frac{k_o t}{2} \cos\theta \right) \right) \oint_c (a_n x a_z) \varphi^{(l)}(r) e^{jkr.R} dl \tag{A.12}$$

$$Z_{in} = \sum_m \sum_n \frac{\delta_m^2}{\left[j\omega C + \frac{1}{j\omega L_{mn}} + g_{mn} \right] \left[1 - \frac{m^2}{\chi_{mn}^2} \right]} \left(\frac{J_m(k_{mn}r}{J_m(\chi_{mn})} \right) \tag{A.13}$$

And finally, from (A.14) and (A.15), the radiated fields are

$$E_\theta = \sum_{l=1}^{n} A^{(l)} E_o^{(l)} . a_\theta \tag{A.14}$$

$$E_\phi = \sum_{l=1}^{n} A^{(l)} E_o^{(l)} . a_\phi \tag{A.15}$$

$$E_\theta(\theta,\phi) = \frac{e^{-jk_oR}}{R}\frac{\pi}{\lambda_o}\left[\cos\left(\frac{k_o t}{2}\cos\theta\right)\right].\sum_m\sum_n a_{mn}V_{mn}e^{j(m\pi/2)}\cos(m(\phi-\phi_o)).$$
$$\left[J_{m+1}(k_o a_{mn}\sin\theta) - J_{m-1}(k_o a_{mn}\sin\theta)\right] \tag{A.16}$$

and

$$E_\theta(\theta,\phi) = \frac{e^{-jk_oR}}{R}\frac{\pi}{\lambda_o}\left[\cos\left(\frac{k_o t}{2}\cos\theta\right)\right]\cos\theta\sum_m\sum_n a_{mn}V_{mn}e^{j(m\pi/2)}\sin(m(\phi-\phi_o)).$$
$$.\left[J_{m+1}(k_o a_{mn}\sin\theta) - J_{m-1}(k_o a_{mn}\sin\theta)\right] \tag{A.17}$$

A.2 ANALYSIS OF TRIANGULAR MICROSTRIP PATCH ANTENNA

Triangular patches have been studied, both theoretically and experimentally, they are found to provide radiation characteristics similar to those of rectangular patches, but with smaller size. The simplest of the triangular shapes, it comprises an equilateral triangular conductor on a grounded dielectric substrate. A nearly equilateral triangular patch has been found to sustain circular polarization. The geometry of simplest triangle antenna is shown in Fig A.3.

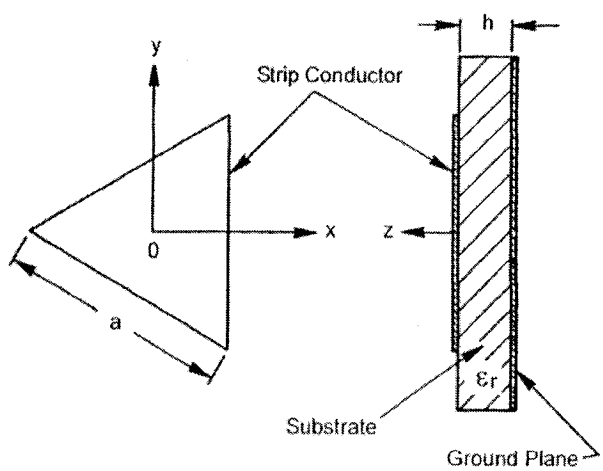

Figure A. 3 Configuration of equilateral triangle microstrip patch antenna.

A.2.1 FIELD REPRESENTATION

The field distribution in a triangular patch can be found using the cavity, in which the triangle is surrounded by a magnetic wall along the periphery as is done for rectangular and circular configurations.

Consider a triangular resonator with magnetic side walls filed with a dielectric material of relativity permittivity ε_r thickness h, since h << λ, there is no variation in the field in the z directions. The solutions for the TE fields in an equilateral triangular have been described by Schelkunoff [48]. By the duality principle, the TM field patterns with magnetic boundary conditions are the same as those for the TE modes with electric boundary conditions, the electric and magnetic field distributions for the TM_{mn} modes can be found as follows [49-52]

$$E_z^{mn} = A_{m,n,l}\psi_{m,n,l}(x,y) \tag{A.18}$$

$$H_x^{mn} = \frac{j}{\omega\mu}\frac{\partial E_z^{mn}}{\partial y} \tag{A.19}$$

$$H_y^{mn} = \frac{-j}{\omega\mu}\frac{\partial E_z^{mn}}{\partial x} \tag{A.20}$$

$$H_z = E_x = E_y = 0 \tag{A.21}$$

where Ψ_{mn} (x,y) are the eigen functions defined as

$$\psi_{m,n,l}(x,y) = \cos\left(\frac{2\pi x'}{\sqrt{3a}}l\right)\cos\left(\frac{2\pi(m-n)y}{3a}\right)$$
$$+\cos\left(\frac{2\pi x'}{\sqrt{3a}}m\right)\cos\left(\frac{2\pi(n-l)y}{3a}\right)+\cos\left(\frac{2\pi x'}{\sqrt{3a}}n\right)\cos\left(\frac{2\pi(l-m)y}{3a}\right) \tag{A.22}$$

and

$$x' = x + al\sqrt{3} \tag{A.23}$$

Expression (A.22) assumes that the origin of the coordinate system coincides with the centroid of the triangle A m,n,l is an amplitude constant determined by excitation, a is the length of a side of the triangle, and m,n,l are integers which are not zero simultaneously, and satisfy the condition

$$m + n + l = 0 \tag{A.24}$$

The modal fields satisfy the wave equation

$$\left(\frac{\partial^2}{\partial x^2} + \frac{\partial^2}{\partial y^2} + k_{mn}^2\right)E_z^{mn} = 0 \tag{A.25}$$

where

$$k_{mn} = \frac{4\pi}{3a}\sqrt{m^2 + mn + n^2} \tag{A.26}$$

It is seen from (A.26) that interchanging the three digits m,n,l leaves the wave number k m, n and the corresponding resonant frequency unchanged. The field patterns for the first two modes TM_{10} and TM_{11} are shown in Fig A.4, The fields for the TM_{10} are symmetrical around the bisector line The above expressions for the fields are general. The particular case, m=1, n=0, and l=-1, corresponds to the dominant mode, for which the field expressions are

$$E_z^{10} = A_{1,0,-1}\left[2\cos\frac{2\pi x'}{\sqrt{3}a}\cos\frac{2\pi y}{3a} + \cos\frac{4\pi y}{3a}\right] \tag{A.27}$$

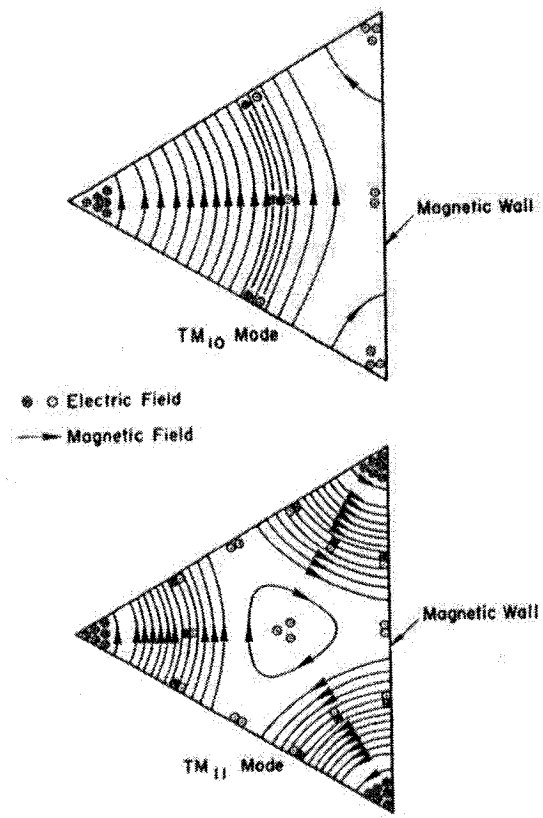

Figure A.4 Field patterns in an equilateral triangular resonator with magnetic walls in TM_{10} mode and TM_{11} mode. [50]

$$H_x^{10} = -jA_{1,0,-1}\xi_o\left[\cos\frac{2\pi x'}{\sqrt{3}a}\sin\frac{2\pi y}{3a} + \sin\frac{4\pi y}{3a}\right] \tag{A.28}$$

$$H_y^{10} = j\sqrt{3}A_{1,0,-1}\xi_o\left[\sin\frac{2\pi x'}{\sqrt{3}a}\cos\frac{2\pi y}{3a}\right] \tag{A.29}$$

where

$$\xi_o = \frac{4\pi}{3a}\frac{1}{\omega\mu}\left(= \frac{1}{120\pi} at\omega = \omega_{1,0,-1}\right) \tag{A.30}$$

A.2.2 RESONANT FREQUENCY

The resonant frequency corresponding to the various modes described by k_{mn} is

$$f_r = \frac{ck_{mn}}{2\pi\sqrt{\varepsilon_r}} = \frac{2c}{3a\sqrt{\varepsilon_r}}\sqrt{m^2 + mn + n^2} \tag{A.31}$$

where c is the velocity of light in free space. The above expressions is valid when the triangular resonator is surrounded by a perfect magnetic wall. The effect of a non perfect magnetic wall on the resonant frequency can be included in an empirical fashion for easy calculation

A number of suggestions have been made with regard to how to modify (A.31) to yield an accurate expression for a triangular microstrip patch antenna that is not enclosed by a prefect magnetic wall, Most of the suggestions are about replacing the side length a by and effective value a_e and leaving substrate dielectric constant unchanged. An expression for a_e has been arrived at by curve fitting the experimental and theoretical results for the resonant frequency for TM10 mode [53]. It is given by

$$f_{10} = \frac{2c}{3a_e\sqrt{\varepsilon_r}} \tag{A.32}$$

APPENDIX B - MOMENT METHOD SOLUTION

B.1 MOMENT METHOD SOLUTION

The moment method solution expands the unknown surface current density on the patch in a set of N expansion or basis modes having unknown complex coefficients I as:

$$J_s = \hat{x}\sum_{nx=1}^{N_x} I_{nx} J_{nx}(x,y) + \hat{y}\sum_{ny=1}^{N_y} I_{ny} J_{ny}(x,y) \qquad \text{(B.1)}$$

where J_{nx} and J_{ny} stand for the known expansion functions or modes, and I_{nx} and I_{ny} are called the unknown complex coefficients. The Fourier transform of these functions given below:

$$F(J_{ni}) = \iint J_{ni} e^{-jk_x x} e^{-jk_y y} dxdy \qquad \text{(B.2)}$$

Equation (B.2) integration is carried out over the range of the nth expansion mode. J_{ni} denotes the Fourier transform of the basis current density.

The inner product with respect to the testing functions J_{ms} is taken in the moment method solution procedure and is given by:

$$\iint_s \vec{E}(\vec{J_e}).\vec{J}_{ms} ds + \iint_s \vec{E}(\vec{J_s}).\vec{J}_{ms} ds = 0 \qquad \text{(B.3)}$$

Application of the Galerkin's procedure, namely the testing function identical to the expansion function, we obtain the matrix equation given as under:

$$[Z]_{NXN}[I]_{NX1} = [V]_{NX1,} N = N_X + N_Y \qquad \text{(B.4)}$$

The impedance matrix elements given in equation (B.4) are given by:

$$Z_{mn} = -\iint_s \vec{J}_m.\vec{E}_n(\vec{J}_n) ds \qquad \text{(B.5)}$$

where E_n stands for the electric field produced by the nth expansion mode J_n. The general form of Z_{mn} taking into account the x and y components of both En and J_m is given as:

$$Z_{mn}^{ij} = -\iint_s \vec{J}_{mi} . \vec{E}_i (\vec{J}_{nj}) ds \tag{B.6}$$

where E_i (J_{nj}) denotes the i-directed electric field produced by the current J_{nj}. E_i is the electric field in the Fourier domain and is given by:

$$\tilde{E}_i (J_{nj}) = \tilde{Z}_{ij} \tilde{J}_{nj} = \tilde{Z}_{ij} F(J_{nj}) \tag{B.7}$$

Substituting equation (B.7) in equation (B.6) after taking inverse transform of equation (B.6), and rearranging the terms, the following expression is obtained:

$$Z_{mn}^{ij} = \frac{-1}{4\pi^2} \int_{-\infty}^{\infty} \int \left(\iint_s J_{mi} e^{jk_x x} e^{jk_y y} ds \right) \tilde{Z}_{ij} F(J_{nj})$$

$$= \int_{-\infty}^{\infty} \int F^*(J_{mi}) Q_{ij} F(J_{nj}) dk_x dk_y \tag{B.8}$$

where

$$Q_{ij} = \frac{-1}{4\pi^2} \tilde{Z}_{ij} \tag{B.9}$$

The block submatrices represent the impedance matrix [Z] in the form given below:

$$[Z] = \begin{bmatrix} \iint F^*(J_{mx}) Q_{xx} F(J_{nx}) & \iint F^*(J_{mx}) Q_{xy} F(J_{ny}) \\ \iint F^*(J_{my}) Q_{yx} F(J_{nx}) & \iint F^*(J_{my}) Q_{yy} F(J_{ny}) \end{bmatrix} dk_x dk_y \tag{B.10}$$

[V] represents the elements for the voltage vector as given below:

$$V_m = \iint_s \vec{E}_s . \vec{J}_m \tag{B.11}$$

where $E_e = E(J_e)$ stands for the electric field produced by the excitation current. The excitation source and the field it forms can be interchanged by employing the reciprocity theorem, and V_m can be expressed as:

$$V_m = \iiint_{excitation} \vec{J_e} \cdot \vec{E_m} d_x d_y d_z \tag{B.12}$$

Suppose that the excitation source is a feed probe positioned at (x_p, y_p). The probe current can be expressed as a filament and can be written as:

$$\vec{J}_e = \hat{z}\delta(x - x_p)\delta(y - y_p) \tag{B.13}$$

E_m is taken to be z directed because J_e is in the z direction and is produced by the mth expansion mode. The general form of V_m can be expressed as:

$$V_m^i = \iiint_{probe} \delta(x - x_p)\delta(y - y_p) E_z(J_{mi}) d_x d_y d_z \tag{B.14}$$

The basis currents give the following expression:

$$\tilde{E}_z(J_{mi}) = \frac{k_i k_2 \cos(k_1 z)}{\omega \varepsilon_o T_m} \tilde{J}_{mi} \tag{B.15}$$

$$\int_0^b \tilde{E}_z(J_{mi}) dz = \frac{k_i k_2 \sin(k_1 h)}{\omega \varepsilon_o k_1 T_m} \tilde{J}_{mi} = \tilde{Z}_{zi} F(J_{mi}) \tag{B.16}$$

where

$$\tilde{Z}_{zi} = \frac{-j\eta_o}{k_o} \frac{jk_1 k_2 \sin(k_1 h)}{k_1 T_m} \tag{B.17}$$

The inverse transform of equation (B.16) is substituted in equation (B.14), and the following expression is obtained:

$$V_m^i = \frac{1}{4\pi^2} \int_{-\infty}^{\infty}\int \left(\iint_s \delta(x - x_p)\delta(y - y_p) e^{jk_x x} e^{jk_y y} dxdy \right) \tilde{Z}_{zi} F(J_{mi}) dk_x dk_y \tag{B.18}$$

$$V_m^i = \int_{-\infty}^{\infty}\int F(J_{mi})Q_{zi}e^{jk_x x}e^{jk_y y}dk_x dk_y \tag{B.19}$$

where

$$Q_{zi} = \frac{1}{4\pi^2}\widetilde{Z}_{zi} \tag{B.20}$$

The voltage vector is given by:

$$[V] = \left[\begin{bmatrix}\iint F(J_{mx})Q_{zx} \\ \iint F(J_{my})Q_{zy}\end{bmatrix}\right]e^{jk_x x}e^{jk_y y}dk_x dk \tag{B.21}$$